

# Mass Transfer in an Energy-Efficient High-Intensity Gas–Liquid Contactor

F. Azizi<sup>†</sup> and A. M. Al Taweel<sup>\*,‡</sup>

<sup>†</sup>Department of Chemical and Petroleum Engineering, American University of Beirut, P.O. Box 11-0236, Riad El Solh, Beirut 1107 2020, Lebanon

<sup>‡</sup>Multiphase Mixing and Separation Research Lab, Department of Process Engineering and Applied Sciences, Dalhousie University, Halifax NS, Canada B3J 2X4

## Supporting Information

**ABSTRACT:** To improve the selectivity and yield of multiphase reactions, an attempt to intensify gas–liquid mass-transfer operations was undertaken in which screen/grid static mixers were used to promote interphase mass transfer. A modified technique was used to enhance the reproducibility of the results and to account for the depletion effect which becomes critical at high mass-transfer rates. The volumetric mass transfer coefficient,  $k_L a$ , was found to increase with increasing liquid superficial velocity and gas volume fraction and reached values as high as  $4.08 \text{ s}^{-1}$  at low specific energy consumption rates, particularly for slowly coalescent systems, a situation that is encountered in most industrially relevant systems. The gas–liquid reactor/contacter presently investigated takes advantage of the coalescence retardation characteristics of most industrially relevant streams to achieve  $k_L a$  values that surpassed those of most conventional reactor/contactors by more than an order of magnitude while maintaining a high energy utilization efficiency (up to  $0.63 \text{ kg O}_2/\text{kWh}$ ). The ability to reach 98% equilibrium within residence times of less than 800 ms, achieved without significantly increasing the power consumption rates, allows for the use of static mixing reactor volumes that are several orders of magnitude smaller than conventional units such as mechanically agitated tanks and bubble columns.

## 1. INTRODUCTION

Gas–liquid mass transfer is the rate-limiting step in a wide range of multiphase chemical and biochemical reactions.<sup>1,2</sup> One of the major goals of intensifying gas–liquid contacting is therefore the enhancement of interphase mass transfer, an objective that could be accomplished by means of providing beneficial concentration profiles in the different phases; enhancing the interphase mass-transfer coefficient,  $k_L$ ; dispersing the gases into fine bubbles that possess large interfacial area of contact,  $a$ ; or by increasing the combined effect of both  $k_L$  and  $a$ . Achieving high volumetric mass transfer coefficients,  $k_L a$ , allows for the use of smaller and safer reactors and can significantly increase the selectivity and yield of mass-transfer-controlled chemical reactions.<sup>3,4</sup> Several contactor types (such as mechanically agitated tanks, bubble-columns, airlift reactors, plunging and impinging jets, reciprocating plate columns, rotor-stators, and oscillatory flow reactors) have been used for this purpose, but the mass-transfer effectiveness significantly varies from one type to another, and the design of such units is very difficult without employing empirical knowledge and experience as well as the use of an extensive amount of pilot-scale testing for scale-up purposes. This is mainly caused by the very complex hydrodynamic conditions prevalent in most of these contactors/reactors where the local value of the mixing intensity, gas holdup, and bubble size distribution exhibit large spatial variations.<sup>5</sup>

Lately, there has been a growing interest in the use of tubular reactors equipped with static mixers as they present an attractive alternative to conventional agitation because of their inherent advantages whereby similar or better perform-

ance can be achieved at lower capital and operating costs. This is highlighted in the findings of several investigations in which high multiphase mass-transfer and reaction rates were achieved in such units in an energy-efficient fashion while simultaneously handling very large flow rates and achieving high heat removal and addition rates.<sup>6–9</sup> Furthermore, the insertion of properly selected static mixing elements into tubular reactors allows for the introduction of the various reactants at different points along the reactor length, thereby facilitating the achievement of optimal temperature and reactant concentration profiles that are required to achieve optimal selectivity and conversion.<sup>7</sup>

Recently, a new type of static mixing element was introduced in which screens/grids are used to repetitively superimpose an adjustable, radially uniform, highly turbulent field on the nearly plug flow conditions encountered in high-velocity pipe flows. The very high energy dissipation rates present in the thin region adjacent to the screen are particularly effective in processing multiphase systems. This is evidenced by their ability to promote contact between different phases, where interfacial areas as high as  $2200 \text{ m}^2/\text{m}^3$  could be efficiently generated in the case of gas–liquid systems.<sup>10</sup> Their ability to promote contact between immiscible liquids was also found to be about 5-fold more energy efficient than mechanically agitated tanks equipped with Rushton-type impellers.<sup>11</sup> The very high grid-generated turbulence and the consequent

**Received:** July 8, 2015

**Revised:** October 29, 2015

**Accepted:** October 29, 2015

**Published:** October 29, 2015

elevated micromixing intensities generated in the regions adjacent to the screens<sup>12</sup> not only result in the formation of fine dispersed phase entities (bubbles and/or drops) but also considerably enhance the value of the interphase mass-transfer coefficient.<sup>13</sup> The combined effect of these two factors resulted in interphase mass-transfer coefficients as high as  $13 \text{ s}^{-1}$  being achieved in the case of liquid–liquid dispersions and allow for 99% of equilibrium conditions to be achieved in less than 1 s residence time.<sup>14</sup> These mixers are also known to exhibit very low axial dispersions.<sup>15</sup>

In a previous study, Al Taweel et al.<sup>16</sup> found that interphase mass transfer can be considerably enhanced by inserting a screen-type static mixing element into the two-phase pipeline flow. In that study, emphasis was placed on achieving significant improvement in interphase mass transfer at low energy expenditures and the elements were therefore placed 375–1175 mm apart. Although that arrangement resulted in significantly enhancing the volumetric mass-transfer coefficient (particularly in the case of slowly coalescent industrial systems simulated by the addition of trace quantities of surfactants), the value of  $k_L a$  was limited to  $0.44 \text{ s}^{-1}$  mainly because of the low energy dissipation rates encountered throughout most of the reactor/contactor volume.

Although such  $k_L a$  values are reasonably high compared to what may be achieved using conventional contactors, they are lower than the mass-transfer rates needed to achieve optimal reaction selectivity and conversion.<sup>7</sup> Consequently, the objective of the present work is to investigate the possibility of using smaller interscreen spacing to achieve even higher volumetric mass-transfer coefficients in gas–liquid systems while maintaining the plug flow characteristics associated with such a design. Furthermore, the effect of the system's interfacial characteristics on the volumetric mass-transfer coefficient achievable in this novel gas–liquid contactor was determined in order to render the findings more relevant to industrial situations.

Virtually all aqueous process streams encountered in the chemical, biochemical, and process industries contain varying concentrations of amphiphilic materials (such as alcohols, surfactants, organic acids, electrolytes, amines, glycols, proteins, and phenols) that are introduced to the system as reactants, as impurities in the feed and recycle streams, or formed as reaction products and/or byproducts. Although it is well-known that the presence of such materials can significantly impact gas–liquid contacting operations, the manner and magnitude by which these changes take place is still controversial. Consequently, much of the practices prevalent today in gas–liquid contacting are based on information and observations obtained using relatively clean systems where the equilibrium between bubble breakage and coalescence is quickly approached, a situation that does not truly reflect what is happening in most industrial situations. Better understanding of the interaction between  $k_L$ ,  $\phi$ , and  $a$  in the presence of amphiphilic material is therefore needed to achieve high energy utilization efficiencies in nonideal real systems. Unfortunately, despite the huge amount of work spent on developing models for drop/bubble breakage and coalescence in turbulent flows, these models cannot be confidently tested and validated because of the scarcity of experimental data obtained under controlled, well-known, and uniform hydrodynamic conditions using actual, or simulated, industrial streams.

The impact of amphiphilic contaminants on gas–liquid contacting of industrial streams can be attributed to the

tendency of such entities to adsorb at the gas–liquid interface and the consequent induction of viscoelastic interfacial characteristics that are very similar to the well-known Marangoni interfacial forces observed in dilute surfactant-containing aqueous solutions.<sup>17</sup> These forces significantly alter the bubble breakage and coalescence rates with the impact being much more pronounced for the latter. For example, Walter and Blanch<sup>18</sup> found that the maximum stable bubble size obtained in turbulently flowing surfactant solutions (pipe flow) increases with increasing interfacial elasticity of the system. Consequently, they modified the classical equation developed by Hinze<sup>19</sup> to account for the need to use greater force to break up bubbles under such conditions. Similar trends were observed by Grau et al.<sup>20</sup> for mechanically agitated tanks in the presence of trace quantities of polyglycols, while the bubble breakage rate constant in the homogeneous turbulent field generated downstream of screens was found to decrease by a factor of about 1.5 in the presence of 2–10 ppm of SDS.<sup>21</sup>

The presence of amphiphilic compounds in water is known to significantly reduce bubble coalescence efficiency in adjacent bubbles<sup>22,23</sup> because of their ability to prolong the time required for the liquid entrapped between the colliding bubbles to drain (film drainage time). That effect is particularly significant in the case of turbulently colliding bubbles where the film drainage time is of the same order of magnitude as the bubble contact time<sup>24</sup> and can thus strongly affect the bubble coalescence efficiency and the coalescence rate. For example, in the PBE simulation of bubble breakage and coalescence in flow downstream from screens/grids, the bubble coalescence rate constant had to be reduced by a factor of 18 in order to match the impact resulting from the addition of 2 ppm of SDS to tap water.<sup>21</sup> That impact is significantly reduced at higher surfactant concentrations where a doubling of SDS concentration resulted in reducing the coalescence rate constant by a factor of 2. This coalescence rate reduction was found to result in the ability to maintain small bubbles for longer times, thereby achieving much larger interfacial area of contact between the phases.

The presence of amphiphilic compounds in aqueous solutions affects not only bubble breakup and coalescence but also interphase mass transfer. When the bubbles move relative to the surrounding liquid, the surface active contaminant entities are transported to the bubble's tailing end where they accumulate, forming a stagnant cap. This reduces internal circulation within the bubble, and the value of the interphase mass-transfer coefficient,  $k_L$ , consequently decreases from that of a circulating bubble to that of a rigid sphere, a phenomenon that represents up to 7-fold reduction in the value of  $k_L$  in the case of 1 mm bubbles.<sup>25–29</sup> Additional reduction is caused by the ability of the Marangoni elasticity to dampen the interfacial and volumetric perturbations,<sup>18,23,25</sup> a factor that plays an important role in determining the magnitude of interphase mass transfer.<sup>17,30</sup> The decrease in the mass-transfer coefficient,  $k_L$ , was also attributed to the surfactants, creating a new resistance to mass transfer due to a change in local diffusion at the boundary layer film.<sup>29,31</sup>

The overall impact that the presence of amphiphilic materials have on the value of  $k_L a$  therefore depends on the counteracting effect they exert on  $k_L$  and  $a$ . Thus, for example, whereas many investigators found that the presence of such materials adversely impacts the volumetric interphase mass-transfer coefficient in a fashion that is dependent on their concentration and interfacial activity as well as the type of

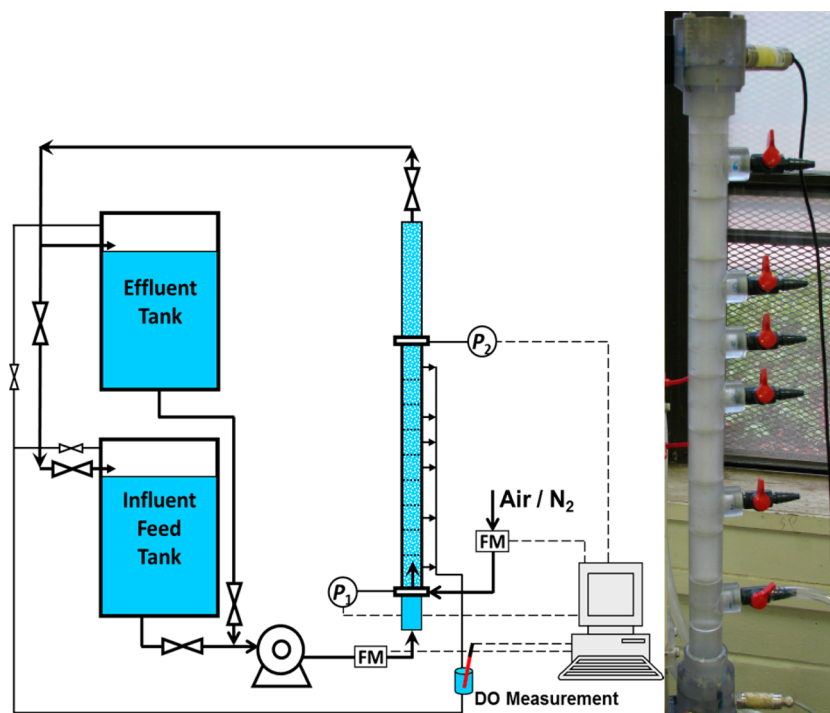


Figure 1. Schematic representation of the experimental setup.

contactor used,<sup>25,26,32,33</sup> others report significant mass-transfer benefits in the presence of coalescence retardation.<sup>8,34–39</sup>

## 2. EXPERIMENTAL SECTION

The steady-state oxygen desorption method was used in this investigation to determine the effect of various hydrodynamic and interfacial factors on the magnitude of the volumetric mass-transfer coefficient achievable using screen-type static mixers. This physical technique was chosen because it does not interfere with the bubble breakage and coalescence processes present in most gas–liquid contactors and can thus be used to investigate the effect of interfacial characteristics. It also does not suffer from the mass-transfer enhancements associated with the chemical techniques.<sup>40</sup> Although this technique was proven to be less sensitive to the effect of oxygen depletion in the case of relatively small mass-transfer coefficients and bubble residence times,<sup>41</sup> a different approach had to be adopted in the present investigation because of the very high mass-transfer coefficients achievable in static mixers and the consequently large changes in oxygen concentration in the gas and liquid phases.

Instead of using the approach used by virtually all previous investigators, in which the dissolved oxygen concentration is measured only in the entering and exiting streams,<sup>42–45</sup> a multipoint measuring approach was used to achieve higher accuracy and reproducibility of the estimated  $k_L a$  value and to decrease its dependence on the mixing pattern within the contactor. Furthermore, the effect of varying oxygen concentration in the gas and liquid phases along the mixer length was accounted for using a mass balance that takes into account the changes in the amount of oxygen present in both the liquid and gaseous streams. This approach overcomes the bias introduced in previous investigations (particularly those obtained at elevated interphase mass-transfer coefficients) as a result of oxygen exhaustion.

**2.1. Experimental Setup.** The continuous flow experimental setup used in the present investigation is schematically depicted in Figure 1. The aqueous phase to be tested was prepared and stored in a 500 L mechanically agitated polyethylene tank from which it was fed to the static mixer loop using a variable speed centrifugal pump (Monarch Industries, model ACE-S20). The flow rate of the liquid phase was measured using a paddle flow meter (Signet model MK 309) and manually varied from 0.4 to 0.96 L/s (which corresponds to liquid superficial velocities,  $U_L$ , in the pipe ranging from 0.8 to 1.9 m/s). The gas phase (compressed air and nitrogen) was injected into the system through a 2 mm L-shaped stainless steel pipe, the tip of which was placed 120 mm upstream of the first screen. The gas flow rate was controlled using a mass flow meter–controller (Aalborg Industries, model GFC 37) in order to achieve the desired gas-to-liquid flow ratios.

Gas–liquid contacting experiments were conducted using a 1200 mm vertical transparent polycarbonate pipe (42 mm OD and 38.1 mm ID) in which the mixing section (560 mm long) was placed 400 mm downstream from the liquid entrance point to ensure radial flow uniformity. The upflow vertical orientation was chosen to eliminate the introduction of multiphase radial nonuniformities caused by the action of gravity and to avoid the formation of the temporal flow nonuniformities reported by Munter.<sup>46</sup>

In this investigation, screen-type static mixing elements (the characteristics of which are given in Table S1) were used because of their ability to generate reasonably uniform hydrodynamic conditions over the whole cross sectional area of the pipe (thereby facilitating the scale-up of the obtained results), their ability to efficiently disperse liquid–liquid and gas–liquid flows,<sup>14,16,21,42,43,46</sup> and their ability to intensify mass-transfer-limited reactions.<sup>8</sup>

The 70-mesh stainless steel woven wire static mixing elements were held apart using a set of transparent

polycarbonate cylindrical spacers (38.0 mm OD and 25.4 mm ID) placed inside the outer pipe (Figure 2). These spacers

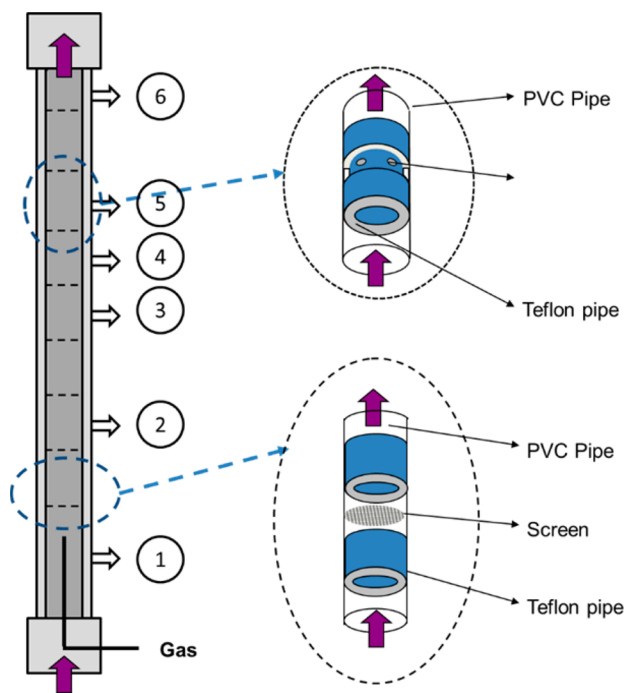


Figure 2. Internal configuration of the contactor/reactor.

ensured that the screens remained perpendicular across the flow direction and maintained the interscreen spacing at the desired value (70 mm in the present investigation). The effective diameter of the mixing section which contains eight static elements is thus 25.4 mm with a total length of 560 mm.

The use of these screen-type static mixing elements resulted in the two-phase being split into about 3800 microjets (70 jets across the diameter) of a length that is dependent on the flow velocity (9.6 mm at the lowest velocity and 4.06 mm at the highest velocity investigated). This, in turn, guarantees that the phases being processed will come into intimate contact with each other and ensures uniform flow condition over the whole cross-sectional area. These characteristics facilitate the scale-up of the experimental results and allows this type of static mixer to be effectively used over a wide range of gas holds with minimum short circuiting.

The setup was provided with five sampling points placed 140 mm apart. At each sampling point, a peripheral ring was provided for withdrawing liquid samples from four circumferential points around the inner pipe (Figure 2), thereby ensuring a more representative sample composition. The oxygen content in the liquid passing through any particular sampling point was measured by continuously withdrawing liquid samples and measuring its oxygen content using a sensitive dissolved oxygen probe (model OD 7685 supplied by B&C Electronics, with a response time of 0.5 s). This ensured that all measurements were performed under steady-state conditions at every sampling point. Additionally, the temperature was monitored using a thermocouple (Cole Parmer Instruments, model 08404-10) while the pressure at the inlet and the outlet of the static mixing section was measured using pressure transducers with a response time of 0.01 s (FP 2000 supplied by Honeywell Sensotec Sensors). The resulting average error in pressure drop measurements was no more

than  $\pm 2.5\%$ . These parameters were used to calculate the mass flow rate of gas necessary to achieve the preset desired gas holdup. This was accomplished using a National Instruments data acquisition board (AT-MIO-16E-10) and a specially developed LabVIEW program.

Although the setup is capable of operating in the recycle mode, all the experiments reported in this investigation were conducted using a once-through approach. Under those conditions, the steady-state oxygen concentrations in the feed stream were typically around  $9.78 \pm 0.25$  ppm and the inlet water temperature was about  $9 \pm 0.5$  °C.

**2.2. Systems Investigated.** In this investigation, the rapidly coalescent air–tap water system was used. However, trace quantities of surface active agents (sodium dodecyl sulfate (SDS) supplied by Sigma Chemical Co.) were added to the aqueous phase to simulate the slowly coalescent behavior of industrial streams and wastewaters.<sup>47–49</sup> This system was selected because of its low volatility and the fact that its static and dynamic interfacial characteristics are well-known; this system is consequently often used to test the effect of interfacial properties on the performance of gas–liquid contactors.

Three different surfactant concentrations were used in the experiments, namely, 0, 10, and 20 ppm (corresponding to 0,  $3.47 \times 10^{-5}$ , and  $6.93 \times 10^{-5}$  M SDS respectively). These concentrations do not alter the bulk properties of water and are much smaller than the critical micelle concentration of  $8.39 \times 10^{-3}$  M.

However, they were found to sufficiently alter the static and dynamic surface tensions as well as the turbulent bubble breakage and coalescence processes particularly for micro-bubbles.<sup>49,50</sup> The bulk properties of these solutions, as well as the static interfacial characteristics, are summarized in Table S2, whereas the range of experimental conditions investigated in this study is summarized in Table S3.

**2.3. Method of Data Analysis.** **2.3.1. Volumetric Mass-Transfer Coefficient.** The steady-state oxygen desorption technique used in this investigation does not require the introduction of any extraneous chemicals which can alter the interfacial characteristics of the system. It can therefore be used to yield accurate estimates of interphase mass transfer for actual, or simulated, industrial streams in which bubble coalescence is retarded. However, it requires a good knowledge of the axial dispersion taking place in the contactor in order to accurately determine the value of  $k_L a$ . Because of the radial uniformity of the hydrodynamic resistance offered by the screen elements, the absence of circular secondary flows that promote bubble segregation, and the large axial resistance offered by the screens, the flow conditions were found to be essentially plug flow in the case of closely spaced screen-type static mixers.<sup>15,51</sup>

The volumetric mass-transfer coefficient was measured using the oxygen/nitrogen/water system, where gaseous nitrogen was fed to the reactor just before entering the mixing section. The nitrogen-rich gaseous stream strips the oxygen from the water stream flowing through the static mixer (nitrogen is thus transferred from the gas bubbles into the liquid while, concurrently, oxygen is transferred from the liquid into the gas bubbles). Under these conditions, the interphase rate of mass transfer can be expressed as

$$\frac{dC_{O_2}}{dt} = -k_L a (C_{O_2} - C_{O_2}^*) \quad (1)$$

where  $C_{O_2}^*$  is the oxygen concentration in the liquid phase at equilibrium with the gases present in the bubbles. Assuming that the volumetric mass-transfer coefficient,  $k_L a$ , to be constant throughout the contactor volume, eq 1 yields the following expression upon integration:

$$\ln(C_{O_2} - C_{O_2}^*) = -k_L a \cdot t + \ln(C_{O_2, \text{in}} - C_{O_2, \text{in}}^*) \quad (2)$$

where  $C_{O_2}$  is the oxygen concentration in the liquid at the sampling point and  $C_{O_2, \text{in}}^*$  and  $C_{O_2, \text{in}}$  represent the initial conditions at the reactor inlet. Because the value of the equilibrium oxygen concentration,  $C_{O_2}^*$ , varies with the location along the contactor/reactor length, its value at every sampling point was determined by a simple mass balance that takes into account the changes of the amount of oxygen present in both the liquid and gaseous streams. Such an approach is necessitated by the very high mass-transfer coefficients and the fact that the exit concentrations in the liquid phase reached up to 70% of the equilibrium value.

To calculate the equilibrium  $O_2$  concentration, the total amount of transferred material was calculated from the measured dissolved  $O_2$  concentration in the liquid phase, and the corresponding partial pressure of  $O_2$  in the gas stream was then determined.

$$C_{O_2}^* = P_{O_2} \times H = \left( P_{\text{sys, local}} \times \frac{n_{O_2, \text{trans}}}{n_{O_2, \text{trans}} + n_{N_2, \text{rem}}} \right) \quad (3)$$

On the basis of that information,  $C_{O_2}^*$  in the liquid was then calculated using Henry's law. The Henry's constant for  $O_2$ , which equals to 769.2 L.atm/mol at 298 K, was corrected for the current operating temperature of 282 K using a van't Hoff equation.<sup>52</sup> Depending on the volumetric flow rates of the aqueous and gaseous phases, the value of  $C_{O_2}^*$  at the outlet was found to vary between 0.28 and 1.17 ppm for the experimental conditions investigated. The  $k_L a$  values predicted using the simplified approach (in which the axial variation of oxygen concentration in the liquid and gas phases is neglected and  $C^*$  is always assumed to be 0 in the gas phase) were found to be 12–35% lower than those determined using the rigorous approach discussed above (average error of 22%). The higher deviations are obtained at elevated mass-transfer coefficients where higher levels of oxygen depletion is encountered.

Assuming that the value of  $k_L a$  remains constant throughout the contactor, a plot of  $\ln(C_{O_2} - C_{O_2}^*)$  versus time should yield a straight line, the slope of which is equal to the volumetric mass-transfer coefficient. As can be seen from the typical results shown in Figure 3, this assumption holds true for the static mixer at hand, and the approach used in this investigation allows for the accurate determination of the mass-transfer coefficient (maximum deviation from the regression line being within  $\pm 5\%$ ) in a fashion that is far superior to that obtained using the two-point approach which relies solely on measuring the inlet and exit concentrations and is thus very sensitive to slight deviations in entry and exit conditions. The reproducibility of the  $k_L a$  results was found to be  $\pm 4.2\%$ .

**2.3.2. Energy Dissipation and Power Consumption.** The pressure drop is the most important design criterion for a static mixer as it is directly related to the energy dissipation rate, which has a decisive role in determining the bubble size distribution of the emerging dispersion and the energy

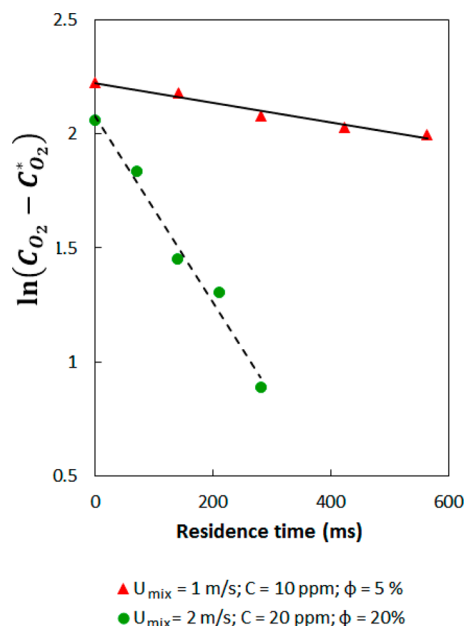


Figure 3. Typical experimental results.

utilization efficiency of static mixers. Three different sources contribute to the overall pressure drop in the reactor at hand, namely, pressure drop due to skin friction at the pipe wall, pressure drop due to the difference in static head caused by the vertical orientation of the mixer, and the pressure drop caused by the flow across the screens. These, in turn, are affected by several operational and design parameters such as the liquid and gas flow rates, the contactor/reactor length, and the number and geometrical configuration of the screen elements used. However, under the highly turbulent conditions encountered in the current study, the pressure drop across the screens is the most dominant parameter where its contribution to the overall pressure drop in the system was found to vary between 70 and 90% depending on the operating conditions.

The volume-average turbulent energy dissipation rate per unit mass of the continuous phase present in the mixer,  $\epsilon$ , is the parameter most commonly used to characterize the hydrodynamic conditions in multiphase mixers and reactors. For inline static mixers, it was calculated from the measured pressure drop values using the following expression:

$$\epsilon = \frac{Q_L \cdot \Delta P}{\rho_L \cdot V_L} = \frac{4 \cdot Q_L \cdot \Delta P}{\rho_L \cdot \pi \cdot D^2 \cdot L \cdot (1 - \phi)} = \frac{U_L \cdot \Delta P}{\rho_L \cdot L \cdot (1 - \phi)} \quad (4)$$

However, it is well-known that the local value of  $\epsilon$  downstream from the screen undergoes dramatic variation along the axis of flow with the maximum value being encountered in the immediate vicinity of the screen.<sup>53</sup> Figure 4 clearly depicts this behavior for the maximum and minimum liquid velocities used in this investigation. It clearly shows that up to 153-fold variation in  $\epsilon$  could be observed within a 7M distance downstream of the screen (corresponding to about 2.5 mm for the screen geometry investigated in this work). Such knowledge of the spatial distribution of the local energy dissipation rate is of great importance when characterizing or designing multiphase contactors/reactors as it plays a crucial role in determining the extent of breakage and coalescence events and is one of the main reasons for the ability to use

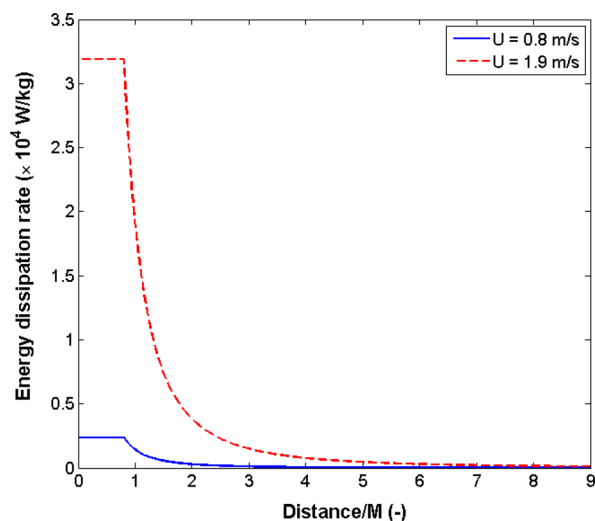


**Figure 4.** Axial variation of local energy dissipation rate per unit mass of the liquid,  $\varepsilon$ , flowing through the screen at the maximum and minimum velocities investigated ( $M = 362.8 \mu\text{m}$ ,  $\alpha = 0.297$ ).

population balance equations (PBE) to model bubble breakage and coalescence in such units.<sup>21,54</sup> The value of  $\varepsilon_{\text{max}}/\varepsilon_{\text{avg}}$  in any particular stage can be as high as 140 which is much higher than those encountered in mechanically agitated tanks (MATs) and impinging jet reactor (IJRs).<sup>55–57</sup> However, whereas complex macromixing flow patterns (that change radically with impeller type and speed) are encountered in the case of MAT, plug flow pattern prevails in the case at hand under all flow conditions, and the decay pattern for the isotropic homogeneous turbulence encountered behind grids and screens is well investigated. Furthermore, the average energy dissipation rate in screen/grid static mixers can easily be changed by altering the interelement spacing. For example, for a  $U_L$  value of 2 m/s, the value of  $\varepsilon_{\text{avg}}$  can be increased from 38 W/kg up to 1890 W/kg by reducing the interelement spacing from 500 mm to 10 mm.

It is interesting to note that the local energy dissipation rates in the microjets generated by the screens,  $\varepsilon_{\text{max}}$ , can be up to 6-fold larger than that encountered in the large jet formed in the ejector throat of the advanced buss loop reactor (32 kW/kg vs 5 kW/kg), a unit which is commonly used to handle very fast gas–liquid reactions as it allows for nearly full conversion in one pass. These microjets are responsible for the breakage-dominated regions observed in conjunction with flow through screens/grids.<sup>10,21</sup> However, the very short liquid residence times encountered in each screen element (varying between 152.75 and 362.4  $\mu\text{s}$  over the range of experimental conditions evaluated) ensures that small bubbles are formed and that high mass-transfer rates are achieved, in an energy efficient manner (section 3.2). Although the microbubbles formed in the microjets will tend to coalesce as they move through the low energy dissipation regions encountered further downstream (Figure 4), the coalescence rate is dependent on the interfacial characteristics of the system, and additional contact time between the phases can thus be provided at relatively high  $k_L$  and  $a$  values without excessive energy dissipation.

Proper understanding of the energy needed to achieve good gas–liquid contacting is constrained by the alternative ways by which the energy input to a mixer (or the rate of energy dissipation) can be characterized. The first approach is related to the overall amount of energy supplied to the mixer per unit

time,  $E$ . This term represents the power input of electric motors driving gas blowers or compressors, liquid pumps, or agitating devices. For the case of in-line static mixers, the following simplified expression can be used to calculate the energy consumption in the contactor/reactor:

$$E = \Delta P \cdot (Q_L + Q_G) \quad (5)$$

The second approach focuses on the rate of energy dissipated per unit time and unit mass in the region where the gas dispersion is formed. The whole dispersion volume is often used if mixing intensity is taken as essentially uniform throughout the contactor volume. This parameter is extensively used to characterize energy demands of various mixer and contactor types. In the case of in-line static mixers, the energy dissipation rate per unit reactor volume is given by

$$E_V = \frac{E}{V} \quad (6)$$

while the energy dissipation rate per unit mass of the gas–liquid dispersion present in the reactor can be written as

$$E_m = \frac{E}{V \cdot \rho_{\text{mix}}} \quad (7)$$

However, these parameters do not truly reflect the energy that has to be provided while processing the immiscible dispersion because they do not take into account the residence time requirements for various mixer and contactor types, a factor which can significantly affect power consumption.<sup>14</sup> To overcome this difficulty, the concept of the energy needed to process a unit of the flowing mixture was applied by Koglin et al.<sup>58</sup> and Al Taweel and Walker<sup>59</sup> to the case of continuously flowing systems. This parameter has the advantage of representing the concerns of mixing equipment users rather than those of equipment designers and has recently been adopted by several investigators.<sup>60,61</sup> It also allows for comparing the performance of mixing units with significantly different mixing times. The energy needed to process a unit of the dispersed phase was thus calculated from

$$E_{\text{spm}} = \frac{E}{V \cdot \rho_{\text{mix}}} \times (\text{residence time}) \quad (8)$$

Alternatively, the overall amount of gaseous matter transferred to or from the liquid phase per unit energy consumed can be used instead of  $k_L a$  to characterize energy effectiveness of interphase mass transport.

The amount of oxygen exchanged between the gas and liquid phases,  $M_{\text{O}_2}$ , is given by

$$M_{\text{O}_2} = Q_L \cdot (C_{\text{O}_2, \text{in}} - C_{\text{O}_2, \text{out}}) \quad (9)$$

while the amount of oxygen transferred per unit power consumption,  $E_t$ , is given by

$$E_t = \frac{M_{\text{O}_2}}{E} \quad (10)$$

This basic parameter,  $E_t$  (units of kg  $\text{O}_2/\text{kWh}$ ), representing the amount of oxygen transported to or from liquid phase per unit of energy consumed, is extensively used in the field of water–wastewater treatment to characterize the effectiveness by which energy is utilized to facilitate interphase mass transport in both the German and U.S. standards.<sup>62,63</sup> However, whereas a standard temperature of 10 °C is used in the German

standards, the U.S. standards use a temperature of 20 °C to more closely reflect the conditions in that country. Because of the large air throughputs used, and the relatively low  $k_L a$  values encountered in water–wastewater aeration devices, variation of oxygen concentration in the gas stream is usually neglected and eqs 9 and 10 simplify to

$$E_t = \frac{k_L a \cdot C_{O_2@10^\circ C}^* \cdot V_L}{E} \quad (11)$$

where  $C_{O_2@10^\circ C}^*$  is the saturation concentration of  $O_2$  in the water at 1 atm and 10 or 20 °C, depending on the standard that is followed. In this study, the values will be reported according to the U.S. standards at 1 atm and 20 °C.

### 3. RESULTS AND DISCUSSION

In this investigation, various operational parameters, as well as the system interfacial characteristics, were varied with the objective of identifying their effect on energy dissipation in the mixer, the volumetric mass-transfer coefficient achieved, and the efficiency by which energy is utilized to facilitate interphase mass transfer. It should be noted that over the whole range of operating conditions, the gas–liquid dispersion remained in the bubbly regime even at the lowest liquid superficial velocities and high dispersed phase volume fractions.

As can be seen from Figure 5, the gas phase was observed to disintegrate into fine bubbles as the two-phase system passes

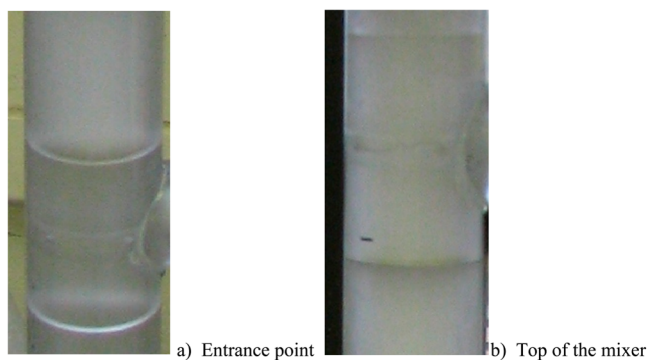


**Figure 5.** Evolution of the G/L dispersion from (a) the entrance to the mixing section to (b) the point where it exits the last screen element ( $U_{\text{mix}} = 1.3$  m/s;  $\phi = 10\%$ ;  $C_{\text{SDS}} = 10$  ppm).

through the first screen-type static mixing element and becomes progressively finer as it passes through subsequent mixing elements. The gas–liquid dispersion was also found to turn more opaque with increasing superficial velocity and/or surfactant concentration. Although no direct measurements of the interfacial area of contact was undertaken in the present investigation, the experimental results reported by Chen,<sup>10</sup> as well as the PBE simulations performed by Azizi and Al Taweel,<sup>21</sup> can be drawn upon to gain better understanding of phenomena taking place because these results cover a situation that is very similar to the one at hand. Depending on the hydrodynamic conditions in the static mixer and the interfacial characteristics of the system investigated, Chen<sup>10</sup> reported that the interfacial areas of contact between the phases increased from less than 200  $\text{m}^2/\text{m}^3$  to more than 2550  $\text{m}^2/\text{m}^3$  as the gas–liquid dispersion passed through successive static mixing elements. This corresponds to the Sauter mean bubble diameter decreasing from 2000 to 165  $\mu\text{m}$  while passing

through the mixer, which compares favorably with the values reported by Heyouni et al.<sup>44</sup> where bubble sizes varied between 900 and 2000  $\mu\text{m}$ .

**3.1. Energy Dissipation Rate.** As previously stated, the pressure drop is the most important criterion in characterizing static mixers as it determines the value of the energy dissipation rate in the system. As can be seen from Figure 6, the pressure

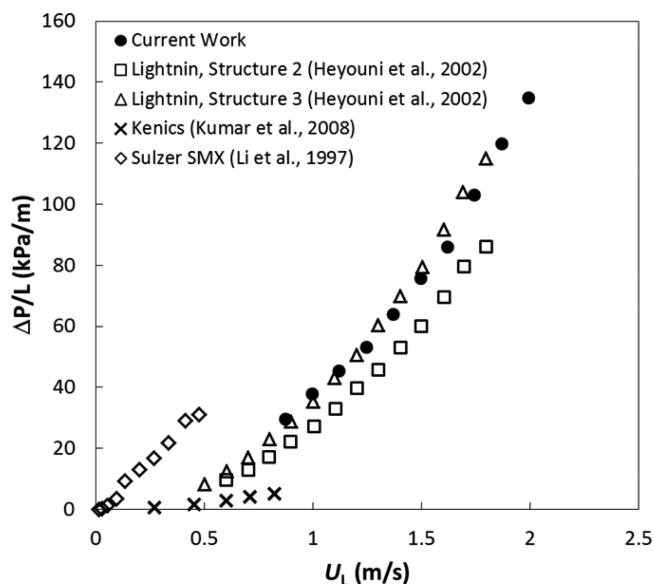


**Figure 6.** Effect of  $U_L$  on the single-phase pressure drop per unit length of various static mixer configurations.

drop per unit length of the screen-type static mixer used in this investigation increases as the liquid superficial velocity is increased. Typically, the pressure drop across the screen is caused by the contribution of both viscous and inertial resistances where the viscous resistance usually dominates in the laminar flow region (i.e., skin friction at the surface of the screen wires). At higher superficial liquid velocities, the effect of the viscous forces become relatively unimportant and the pressure losses result mainly from the turbulent vortices associated with the sudden contraction and expansion caused by the presence of screen/grid across the flow path.<sup>53</sup>

It is therefore interesting to note that the single-phase pressure drop per unit length of the mixer (necessary to unify residence times in the various designs) associated with the use of the present screen-type static mixer in single-phase flow is not significantly different from that reported by Heyouni et al.<sup>44</sup> for structure 3 of the Lightnin static mixing elements (alternating right-hand and left-hand elements), but it is significantly smaller than those reported for the Sulzer SMX mixer.<sup>64</sup> On the other hand, they are higher than those associated with the use of less disruptive element configurations such as Kenics mixers<sup>65</sup> or structure 1 or 2 of the Lightnin static mixing elements.

The introduction of the gas phase to a liquid flowing at any particular liquid superficial velocity,  $U_L$ , reduces the gas–liquid dispersion density,  $\rho_{\text{mix}}$  but increases its superficial velocity ( $U_{\text{mix}} = U_L + U_G$ ). Consequently, the kinetic energy of the microjets formed by the screen were found to increase by a factor of up to 25%; however, contrary to the results obtained by several previous investigators,<sup>42,44,66</sup> no significant increase in the pressure drop across the static mixer was observed in the present investigation (Figure 7a).

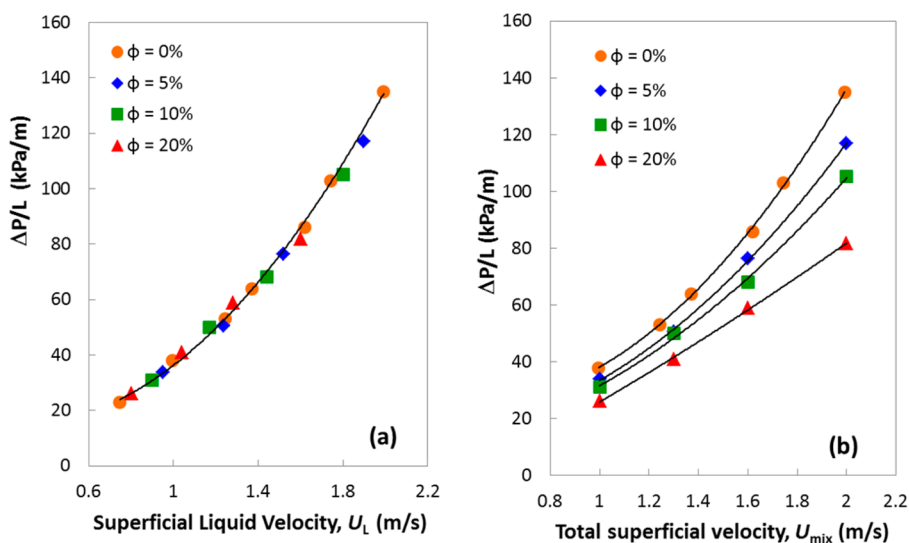


**Figure 7.** Effect of the gas holdup on the pressure drop per unit length of the mixer: (a) pressure drop versus liquid-phase velocity and (b) pressure drop versus mixture velocity (air–water).

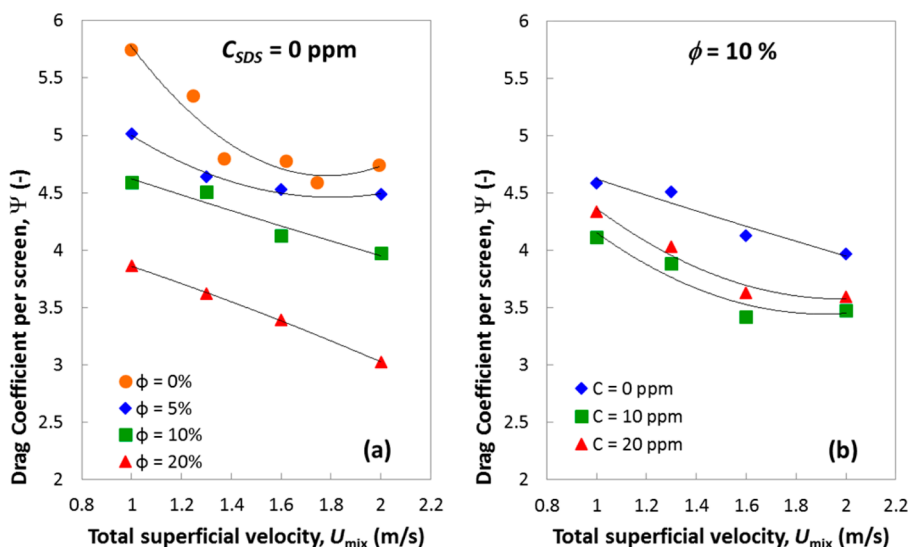


**Figure 8.** Effect of gas holdup (a) and SDS concentration (b) on the drag coefficient of screens.

This difference is most probably caused by the formation of much finer bubbles in the present investigation and is in line with the recent observations reported by Parmar and Majumder<sup>67</sup> where the drag coefficient in two-phase pipe flow was found to decrease with increasing surfactant concentration and the consequent formation of finer bubbles. This is clearly illustrated by the observation that, at any particular dispersion superficial velocity, the pressure drop across the contactor was found to decrease upon the introduction of the gaseous phase with the effect being more pronounced as the volume fraction of the gas increased (Figure 7b). This is partially caused by the lowering of dispersion density (which is inversely proportional to the gas-to-liquid flow ratio) and the consequent reduction in the kinetic energy of the microjets formed by the screen.<sup>53</sup> This factor, however, could not fully account for the pressure reductions observed, and the remaining difference may have been caused by the reduced drag coefficient of screens which was observed to take place in the presence of fine bubbles in the flowing stream.<sup>10</sup> This drag reduction phenomenon is mainly caused by the

ability of microbubbles to modulate the turbulence structure in multiphase flows,<sup>68,69</sup> a phenomenon that is being taken advantage of to reduce drag on ship hulls and pipelines.<sup>70,71</sup> However, the increased compressibility of the gas–liquid dispersion (which is more pronounced at higher gas-to-liquid ratios) could also be allowing for a higher recovery of the inertial losses when the two-phase mixture passes through the screens (another mechanism for reducing the drag and total pressure losses).

The ability of microbubbles to reduce the drag coefficient,  $\Psi = \Delta P / ((1/2)\rho U^2)$ , for flow through screens is clearly shown in the results depicted in Figure 8 where 36% drag reduction was observed when 20% gas was introduced into tap water. This impact is intensified in the presence of SDS mainly because of the formation of finer microbubbles. These observations are significantly different from those reported for pipe flow<sup>67</sup> and can be partially attributed to the ability of screen/grid static mixing elements to effectively disperse the gas phase into microbubbles even when tap water is used. (It is commonly overlooked that tap water typically contains small amounts of

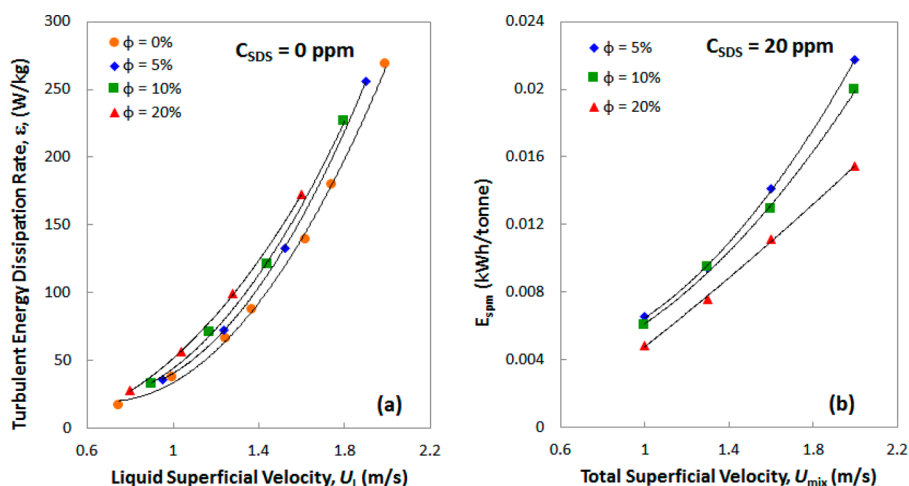


**Figure 9.** Effect of gas holdup on (a) the average rate of turbulent energy dissipation in the liquid phase,  $\varepsilon$ , and (b) the specific energy consumption per unit mass processed.

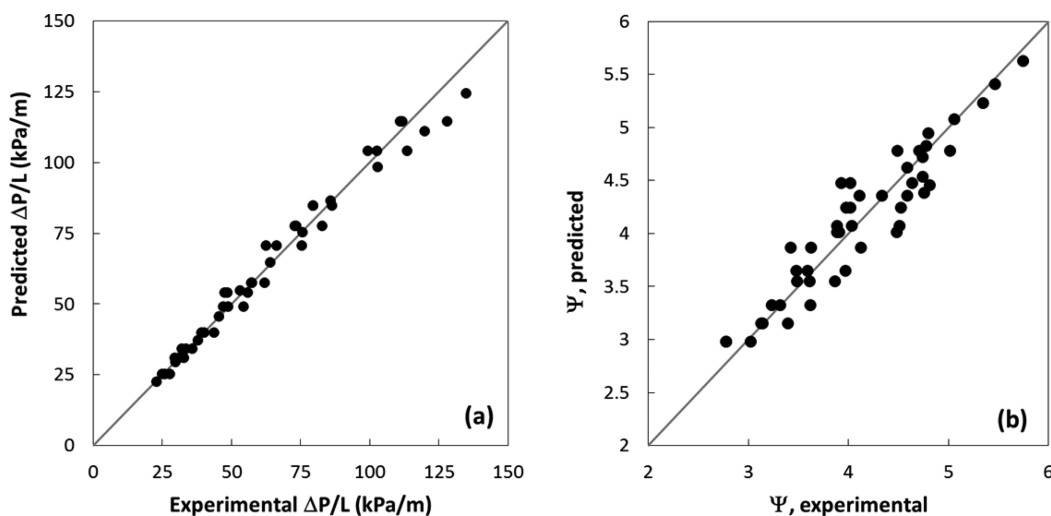


**Figure 10.** Parity plot of predicted versus experimental results for the (a) pressure and (b) drag coefficient of the screen.

electrolytes and traces of natural and synthetic amphiphilic compounds, the presence of which can strongly affect interphase mass transfer and bubble coalescence.<sup>30</sup>) The fact that the boundary layer thickness for flow across orifices is much smaller than that for pipeflow could be another contributor to the anomalous behavior. The addition of trace quantities of SDS to the tap water facilitates the formation and stabilization of microbubbles and hence resulted in increasing the reduction effect up to a maximum of 41.6.

On the other hand, as can be seen from the results shown in Figure 9a, the average turbulent energy dissipation rate in the liquid phase,  $\varepsilon$ , was found to slightly rise with increasing gas holdup. Such a behavior is expected to enhance the volumetric mass-transfer coefficient because the elevated  $\varepsilon_{\text{avg}}$  values will result in increasing the bubble breakage frequency (resulting in the formation of higher specific interfacial area of contact,  $a$ ) while the mass-transfer coefficient,  $k_L$ , would also be improved. However, such an increase in the liquid-phase turbulent energy dissipation was not reflected in a proportionate increase in the power consumption rates. As can be seen from Figure 9b, the specific power consumption per unit mass of the liquid phase processed through the mixer was found to decrease as the dispersed phase volume fraction increased. Whereas a

significant part of this reduction in the value of  $E_{\text{spm}}$  emanates from the reduction in the total pressure drop associated with increasing  $\phi$ , most of it stems from the shorter residence times associated with the larger total superficial velocities.

The pressure drop data obtained in the present investigation (49 points) were correlated and good agreement (average deviation of 4.68%) was achieved between the predicted values (obtained using eq 12) and the experimental data (Figure 10a).

$$\Delta P = 20.9 \times U_{\text{mix}}^{1.75} \times (1 - \phi)^{1.73} \quad (R^2 = 0.986) \quad (12)$$

To highlight the phenomenon of drag reduction encountered by bubbly two-phase flow through screens, the screen drag coefficient was correlated in a fashion similar to that proposed by Ehrhardt<sup>72</sup> and Chen<sup>10</sup> where the drag coefficient is given as a function of the screen open area,  $\alpha$ , and the wire Reynolds number,  $Re_b$  ( $Re_b = (b \cdot U_{\text{mix}} \cdot \rho_{\text{mix}}) / \mu$ ). However, the term  $(1 - \phi)$  was introduced to account for the drag reduction effect that the presence of microbubbles have on the drag coefficient of screens. As can be seen from the parity plot depicted in Figure 10b, the drag coefficient correlation presented by eq 13 yields reasonably good correspondence (average deviation of 4.7%) with the experimental results.

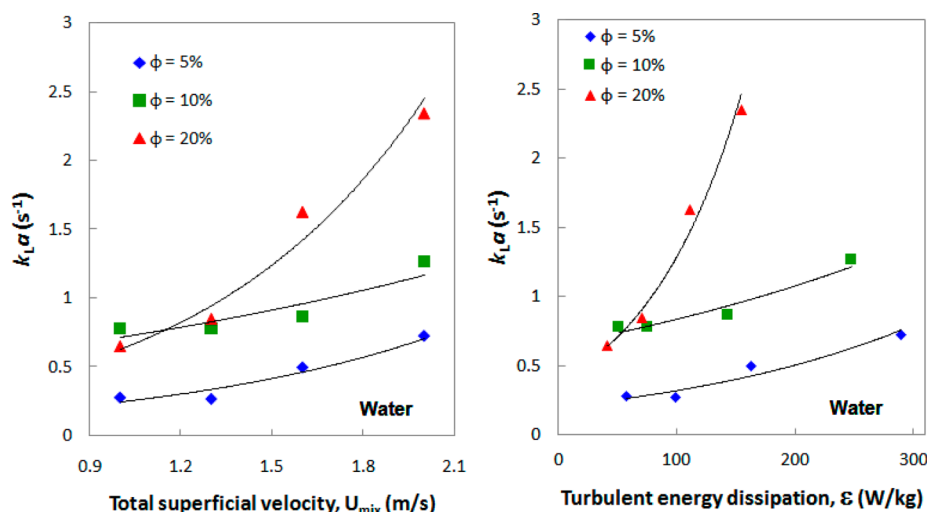


**Figure 11.** Effect of the total superficial velocity and the turbulent kinetic energy dissipation rate on the volumetric mass-transfer coefficient obtained in the air–water system.

$$\Psi = \frac{3.264}{(\text{Re}_b/\alpha)^{0.254}} \cdot (1 - \phi)^{1.732} \cdot \left(\frac{1 - \alpha}{\alpha^2}\right) \quad (R^2 = 0.887) \quad (13)$$

**3.2. Volumetric Mass-Transfer Coefficient.** In a previous study, Al Taweel et al.<sup>16</sup> found that the mass transfer in two-phase pipe flows is considerably enhanced by introducing screen-type static mixing elements into the pipeline. Although high energy utilization efficiencies were achieved by introducing one or two screen elements placed 1.175 m apart, the resulting volumetric mass-transfer coefficient was limited to relatively low values ( $k_L a < 0.44 \text{ s}^{-1}$ ). Such contacting arrangement will therefore be most suitable for use in processing operations where energy expenditures are of primary importance (e.g., wastewater aeration, the stripping of volatile compounds, and advanced oxidation processes) or for conducting relatively slow multiphase chemical reactions where selectivity and/or process safety necessitate the use of slower reaction and mass-transfer rates (e.g., highly exothermic reactions, oxidation of trace compounds, disinfection by uncatalyzed ozonation). On the other hand, the ability to achieve high volumetric mass-transfer coefficients plays a significant role in enhancing the conversion, selectivity, and inherent safety of many fast multiphase reactions.<sup>7</sup> The present investigation therefore focuses on the potential for achieving high volumetric mass-transfer coefficients by using closely spaced screen-type static mixing elements. Emphasis was placed on the effect of superficial liquid velocity, the gas-to-liquid flow ratio, as well as the interfacial characteristics of the system where the latter plays a particularly significant role in industrially relevant systems.

**3.2.1. Effect of Superficial Liquid Velocity.** The superficial velocity of liquids and gases flowing through a static mixer controls the residence time of the continuous and dispersed phases in the mixer as well as the characteristics of the turbulence field generated within the mixer (intensity, characteristic length, and energy dissipation rate). For the particular design at hand, this applies to both the relatively small levels of turbulence generated by the pipe flow section between the mixing elements as well as the much larger energy dissipation rates generated as the gas–liquid dispersion flows through the screen-type static mixing elements.<sup>21</sup> All of these factors play an important role in determining the mass-transfer

coefficient,  $k_L$ ; the bubble size distribution; and the interphase rate of mass transfer in the rapidly coalescent gas/water system.<sup>73</sup> Recently, however, there has been a growing effort aimed at understanding the interaction between these parameters in slowly coalescent systems which are of greater importance to the industrially relevant systems as well as those that occur in nature (e.g., lake water and marine environments, wastewater treatment).<sup>27,33,74</sup>

As previously mentioned, an increase in the liquid superficial velocity results in increasing the pressure drop and  $\epsilon$  in both the narrow microjet regions adjacent to the screens/grids, as well as the average turbulent energy dissipation rate throughout the reactor/contacter,  $\epsilon_{\text{avg}}$ . Several investigators<sup>10,21,43</sup> found that when a gas–liquid mixture flows through successive regions of high energy dissipation rates, the bubbles undergo very rapid breakage into microbubbles that provide very large interfacial area of contact between the phases. Consequently, high  $k_L a$  values are expected to be achieved at elevated velocities, particularly because the value of the mass-transfer coefficient,  $k_L$ , will also be enhanced by elevated turbulence levels.<sup>27,75,76</sup>

The results depicted in Figure 11a,b clearly show such behavior where an increase in  $\epsilon_{\text{avg}}$  produces an increase in the value of  $k_L a$  with the impact being more pronounced at elevated gas holdups where the greater coalescence tendencies resulting from the larger bubble population densities are counteracted by the higher shear stresses which favor the formation of fine bubbles and enhance the liquid-side mass-transfer coefficient. Such behavior was observed in the rapidly coalescent air–water system as well as for the slowly coalescent surfactant-containing systems.

**3.2.2. Effect of Gas-to-Liquid Flow Ratio.** At any particular energy dissipation rate, an increase in gas holdup results in increasing the bubble population density which, in turn, enhances bubble collision and coalescence rates and shifts the bubble breakage–coalescence equilibrium toward the formation of larger bubbles. Consequently, the interfacial area of contact between the phases does not necessarily increase in proportion to the gas holdup unless coalescence is completely suppressed. However, under conditions where coalescence can take place, the impact of increasing gas holdup on mass transfer depends on the two counteracting influences, and the overall

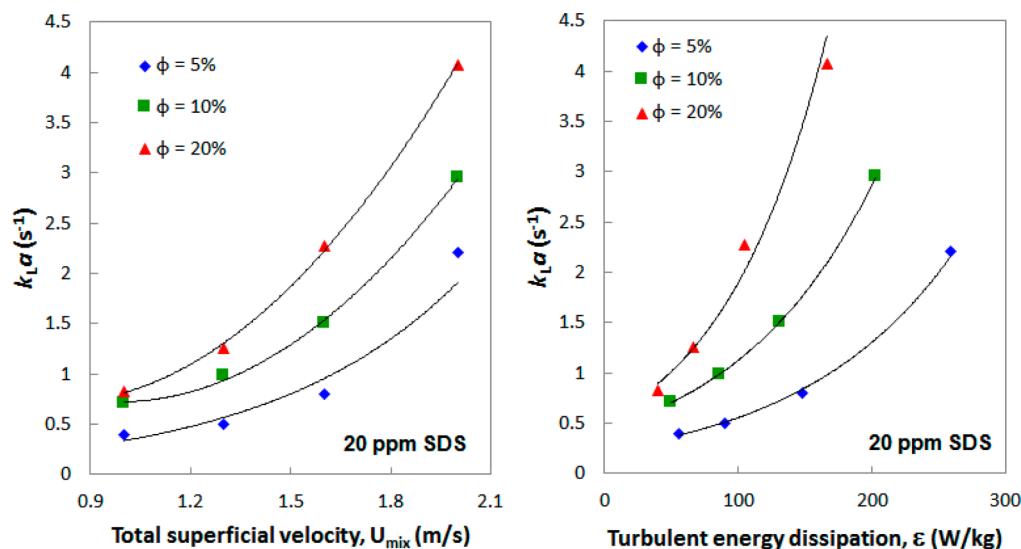


Figure 12. Effect of gas-to-liquid flow ratio on the volumetric mass-transfer coefficient in air–water system containing 20 ppm of SDS.

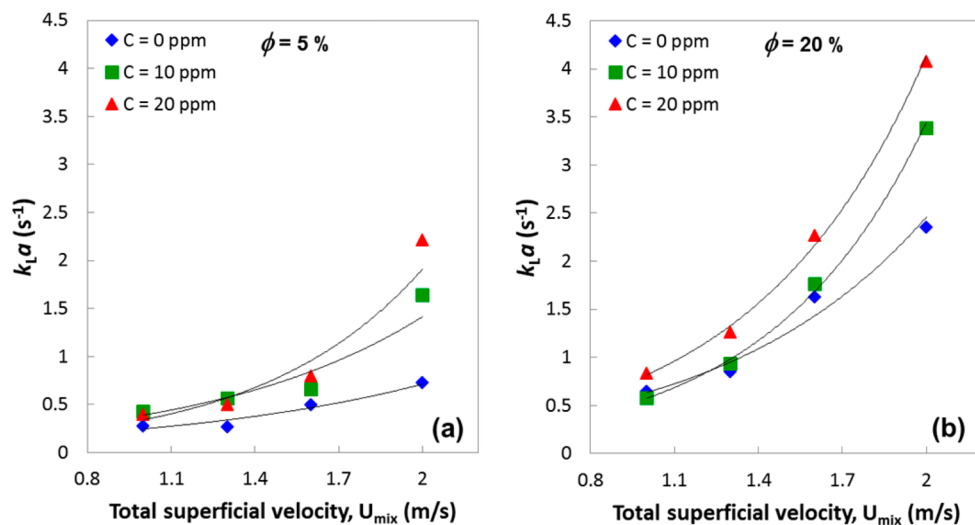


Figure 13. Effect of SDS concentration and gas holdup on the average volumetric mass-transfer coefficient (a)  $\phi = 0.05$  and (b)  $\phi = 0.2$  (70 mm interscreen spacing).

impact is determined by the net impact of the interfacial area of contact,  $a$ , and the indirect effect on the value of  $k_L$ .

Because of the formation of very small bubbles throughout the range of experimental conditions investigated in this study, their small slip velocity can be neglected relative to the very high liquid velocities investigated and the gas-to-liquid flow ratio can be considered as essentially equal to the gas holdup,  $\phi$ . The impact of gas holdup on the average volumetric mass-transfer coefficient is clearly evident in Figures 11 and 12, which depict the results obtained for the rapidly coalescent air–water system as well as those obtained using the virtually noncoalescent system which contains 20 ppm of SDS.

This can be attributed to the greater bubble coalescence tendencies in the case of air–tap water which result in the interfacial area of contact being less than proportional to the gas holdup. This is clearly illustrated by the observation that in the case of the rapidly coalescent air–tap water system a doubling of the gas holdup (from 10 to 20%) results in no significant increase in the mass-transfer coefficient at energy dissipation rates less than 110 W/kg, while the slight lowering

in the  $k_L a$  value (observed at the lowest velocity) may have been caused by the presence of an increasing number of neighboring bubbles and its subsequent effect on mass transfer.<sup>75</sup>

These trends are in line with the experimental findings of Chen<sup>10</sup> and the population balance simulations of Azizi and Al Taweel,<sup>21</sup> who reported an enhancement in the interfacial area of contact with an increase in the gas holdup for the case of gas–liquid dispersions turbulently flowing through screens/grids. The fact that increasing turbulence intensity positively influences both  $k_L$  and  $a$  results in the cumulative effect on both factors ( $k_L a$ ) depicting an exponential behavior (Figure 11b).

The effect of gas holdup on the volumetric mass-transfer coefficient,  $k_L a$ , is often taken into account by investigating the factors affecting the volumetric mass-transfer coefficient per unit volume of the gas present in the reactor/contact,  $k_L a/\phi$ . This parameter was found to correlate the mass-transfer performance of gas–liquid reactor types reasonably well with a particular emphasis on the effect of bubble size.<sup>77–80</sup> Whereas several investigators reported that this parameter varies slightly

over a wide range of operating conditions for bubble columns and vibrating monolith reactors ( $k_L a / \phi = 0.5\text{--}1.5$ ),  $k_L a / \phi$  values as high as 45 were achieved using the static mixer at hand,<sup>81</sup> a factor that makes this contactor type well suited for handling very fast chemical reactions such as oxidation, halogenation, hydrogenation, and hydroformylation.

**3.2.3. Effect of Interfacial Characteristics.** Although the presence of small quantities of SDS is expected to somewhat decrease the maximum stable bubble size (due to the reduction of static surface tension), this tendency is counteracted by the tendency to impede bubble breakage due to the development of the Marangoni elastic forces.<sup>18</sup> On the other hand, bubble coalescence rate is strongly hindered by the presence of very small SDS concentrations.<sup>49,82</sup> Consequently, the fine bubbles generated at the screen/grid mixing elements will be maintained for longer distances downstream, thereby yielding high specific interfacial areas which should enhance the value of the volumetric mass-transfer coefficient. This was experimentally confirmed by Chen<sup>10</sup> and by the population balance simulation results undertaken by Azizi and Al Taweel.<sup>21</sup> However, as mentioned previously, the presence of SDS negatively affects the liquid-phase mass-transfer coefficient,  $k_L$ , because of its ability to induce viscoelastic properties at the gas–liquid interface.<sup>30</sup> The effect of SDS concentration on the average volumetric mass-transfer coefficient is therefore a function of the overall effect of these competing factors.

The results obtained in this investigation clearly show that in the case of closely placed screen/grid static mixing elements, the value of  $k_L a$  increases with an increase in the SDS concentration (Figure 13) with the magnitude of the increase being most prominent at higher surfactant concentrations and high energy dissipation rates. This observation suggests that under the conditions used in this investigation, the reduction in the value of the interphase mass-transfer coefficient caused by the presence of the surfactants does not outweigh their ability to retard the coalescence rate and maintain the large interfacial area generated by the screens/grids for a long distance (thereby increasing the average interfacial area of contact between the phases). Similar observations have been reported by Jackson<sup>83</sup> and Zlokarnik<sup>34</sup> who investigated the mass-transfer behavior of different industrial streams. Furthermore, these findings are in line with those reported by Al Taweel et al.<sup>16</sup> in which one or two screen-mixing elements were introduced in a pipe flow to enhance the mass-transfer performance of the contactor. However, in their study, the volumetric mass-transfer coefficient was found to increase with an increase in the SDS concentration up to 10 ppm and then decreases as the surfactant concentration increased further. This anomalous behavior could be attributed to the low levels of energy dissipation rates used in the previous investigation where the mixing elements were placed 775–1175 mm apart ( $0.04 < \varepsilon_{\text{avg}} < 1.6$  W/kg), whereas average turbulent energy dissipation rates as high as 310 W/kg were achieved in the present investigation by placing the elements 70 mm apart.

The impact of interscreen spacing, and the associated change in average energy dissipation rates, on interphase mass transfer can be best illustrated by the observation that whereas  $k_L a$  values as high as  $0.44 \text{ s}^{-1}$  were observed in the work of Al Taweel et al.<sup>16</sup> in the presence of 10 ppm of SDS,  $k_L a$  values as high as  $3.4 \text{ s}^{-1}$  were observed in the current work for the same level of contamination and superficial velocities.

These observations stand in contrast to the findings of several investigators where the presence of anionic or cationic

surfactants in the system was found to significantly reduce the value of the volumetric mass-transfer coefficient.<sup>23,28,31,84–86</sup>

This anomaly can be mainly attributed to the ability of screen/grid static mixing elements to focus energy dissipation rate within a small volume and the reliance on the coalescence retardation ability of surfactant-containing solutions to maintain large interfacial area of contact in regions of low energy dissipation rates.

**3.3. Correlating the Volumetric Mass-Transfer Coefficient.** As shown above, the volumetric mass-transfer coefficient achieved in screen/grid static mixers was found to be affected by the energy input to the system, the gas holdup, and the interfacial characteristics of the system. Attempts were therefore made to correlate the overall volumetric mass-transfer coefficient obtained under the highly turbulent conditions used in this investigation with the various operating conditions affecting it.

For design purposes, the data obtained were correlated using a simple correlation that is often used in the case of static mixers:

$$k_L a = A \cdot U_L^a \cdot U_G^b \quad (14)$$

The values of  $a$  and  $b$  obtained for the range of experimental conditions given in Table S3 ( $a = 1.15$  and  $b = 0.75$ ) clearly show that the liquid velocity has an impact on  $k_L a$  that is stronger than that of the gas velocity and are in line with previous investigations in which, depending on the type of static mixer used, these exponent vary between  $a = 1.5\text{--}1.8$  and  $b = 0.53\text{--}1.0$ .<sup>44,46</sup>

To develop better understanding of the mechanisms responsible for the good mass-transfer performance achieved in screen/grid static mixers, and to facilitate comparison with other contactor types, an approach similar to that adopted for in-depth analysis of mechanically agitated tanks and static mixers was adopted. In this approach, the  $k_L a$  data are usually correlated using the following format:

$$k_L a = \alpha \cdot \varepsilon^\beta \cdot \phi^\gamma \quad (15)$$

However, by changing the concentration of SDS in water, it was also possible to conduct experiments at three levels of bubble coalescence retardation, which allows for the introduction of a third correlation parameter that acts as an indicator of the bubble coalescence tendency.

$$k_L a = \alpha \cdot \varepsilon^\beta \cdot \phi^\gamma \cdot \sigma^\delta \quad (16)$$

To facilitate comparison with the correlations obtained by other investigators, the results obtained for each gas–liquid system were separately analyzed followed by an analysis of the whole set of data (36 points) where the static surface tension was introduced as an indicator of the ability of SDS to affect coalescence retardation tendencies and reduce the value of  $k_L$ . The resulting regression values for the four parameters are given in Table 1.

**Table 1. Mass-Transfer Correlation Parameters**

liquid stream	$\alpha$	$\beta$	$\gamma$	$\delta$
air–water	0.524	0.50	0.83	–
air–water + 10 ppm of SDS	0.125	0.738	0.49	–
air–water + 20 ppm of SDS	0.13	0.84	0.66	–
all points	0.0018	0.68	0.66	–1.69

For the rapidly coalescent air–tap water system, the value of  $\beta = 0.50$  is smaller than that typically reported for other static mixer configurations where it was found to vary between 0.7 and 1.0.<sup>42,44,46,87</sup> It is however very close to the value recently reported for MAT ( $\beta = 0.57 \pm 0.15$ ) as well as that for the vertical Corning advanced flow reactor.<sup>88,89</sup> The values obtained for  $\gamma$  in the present investigation are within the range reported in the literature for static mixers handling the rapidly coalescent air–water system, where  $\gamma$  ranged from 0.6 to 1.<sup>42,44,90</sup> That exponent value is however almost twice that reported in conjunction with the vertical Corning advanced flow reactor, where  $\gamma = 0.46$  for rapidly coalescent systems.

In a fashion similar to that reported by Linek et al.<sup>88</sup> and Moucha et al.,<sup>74</sup> the value of  $\beta$  was found to progressively increase with decreasing coalescence tendencies, reaching  $\beta = 0.84$  in the presence of 20 ppm SDS. However, because of the uniform distribution of gas holdup throughout the volume of screen-type static mixers, the value of  $\beta$  obtained in this investigation is slightly less than that reported by Linek et al.<sup>88</sup> for slowly coalescent 0.5 M Na<sub>2</sub>SO<sub>4</sub> solution in the highly nonuniform MAT (where  $\beta = 1.10 \pm 0.17$ ). This trend suggests that the efficiency by which energy is utilized to promote interphase mass transfer is improved as the surfactant concentration is increased in spite of the well-known adverse effect that the presence of surfactants has on  $k_L$ .<sup>17,30,31</sup> This, in turn, suggests that the overall impact of increasing coalescence retardation on the  $k_L a$  value achievable in appropriately designed contactors is controlled by the enhanced generation of interfacial area of contact between the phases rather than by the reduction in the value of  $k_L$  usually associated with the presence of coalescence-retarding agents such as electrolytes and surfactants.

As can be seen from Figure 14, good agreement between predicted and experimental results was achieved ( $R^2 = 0.87$

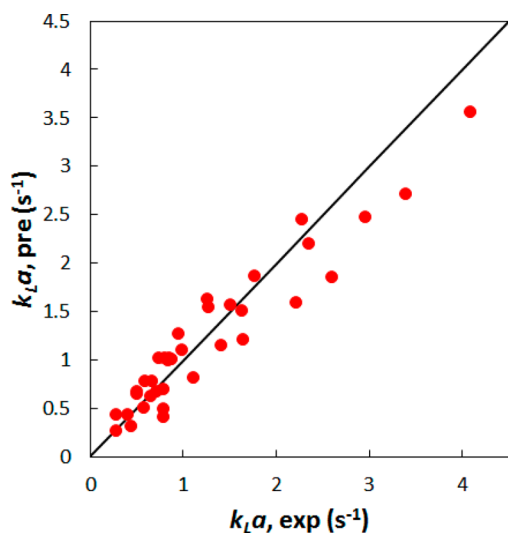


Figure 14. Parity plot of  $k_L a$  values predicted using eq 17 against experimental results.

with average deviation of 18.4%) using the general correlation which can be applied to systems with a wide range of interfacial characteristics:

$$k_L a = 0.0018 \cdot \varepsilon^{0.68} \cdot \phi^{0.66} \cdot \sigma^{-1.69} \quad (17)$$

It is interesting to note that the value of  $\beta = 0.68$  obtained using the whole data set (including various degrees of coalescence rates) is very close to that predicted by Kolmogorov's inertial range hypothesis, whereas the value of  $\gamma$  is well within the range of values reported by other investigators for MATs and static mixers.

Although the static surface tension provided a good indication of how the presence of SDS affects the coalescence retardation tendencies and reduces the value of  $k_L$ , it is necessary to investigate this phenomenon in greater depth to identify the physically relevant static and/or dynamic interfacial parameters responsible for enhancing the improvement in the volumetric mass-transfer coefficient in highly turbulent gas–liquid contactors.

**3.4. Comparison with Other High-Rate Gas–Liquid Contactors.** As can be seen from the results shown above, as well as those presented by Al Taweel et al.,<sup>16</sup> a very wide range of interphase mass-transfer rates can be achieved by using screen/grid static mixing elements and varying the three main design and operating conditions, namely, superficial liquid velocity, gas-to-liquid flow rate ratio, and the interelement spacing. However, the previous investigation focused on high energy utilization efficiencies particularly in the case of slowly coalescent systems that are of industrial significance; the value of  $k_L a$  was limited to 0.44 s<sup>-1</sup> mainly because of the low energy dissipation rates encountered throughout most of the reactor/contactor volume at large interelement spacing. On the other hand, the present investigation focused on achieving high interphase transfer rates in order to enhance the yield and selectivity of fast gas–liquid reaction. Comparison with other contactors will therefore focus on reactor types that can achieve high transfer rates, such as microchannel reactors, impinging jet reactors, spinning disc reactors, monolith loop reactors, Corning's advanced flow reactors, static mixers, and MATs. The most relevant hydrodynamic and mass-transfer parameters for gas–liquid contacting in these units are given in Table 2 where the units are organized in ascending capacity to handle large process stream throughputs.

Achieving high interphase mass-transfer rates is one of the main objectives of gas–liquid contacting because it significantly affects the reaction rate, yield, and selectivity; the reactor volume; as well as the intrinsic safety of the operation. This, however, necessitates the expenditure of energy to enhance the value of  $k_L a$ , which usually increases as a function of the local energy dissipation rate,  $\varepsilon$ . The effectiveness by which this is accomplished can, however, vary significantly from one contactor design to the other because the efficiency by which energy is utilized to promote interphase mass transfer is strongly influenced by the flow patterns of the liquid and gas phases within the contactor and the residence times within the high energy dissipation regions.<sup>81</sup>

Whereas extremely high specific surface areas and overall mass-transfer coefficients can be achieved in gas–liquid microchannels (Table 2), the throughputs that can be achieved are not sufficient for large-scale applications and limit their use to the production of small quantities of specialty chemicals. The use of a rotor–stator spinning disc reactor allows for higher throughputs at the expense of lower  $k_L a$  values and order-of-magnitude higher energy dissipation rates. In this design, the volumetric mass transfer is promoted by the surface renewal of the liquid film between a large bubble and the rotor or the stator which is enhanced when small gaps are used. A similar approach is utilized in Corning's advanced flow reactor which is

Table 2. Mass-Transfer Characteristics of High-Rate Gas–Liquid Contactors

contactor type	liquid flow pattern	$\epsilon_{\text{avg}}$ (W/kg) <sup>a</sup>	$k_L a$ (s <sup>-1</sup> )	source
microchannel reactor	co-current	N/A	0.3–21	Yue et al. <sup>91</sup>
rotor–stator spinning disc reactor	fully mixed	100–6000	0.02–0.43	Meeuwse et al. <sup>92</sup>
advanced flow reactor	co-current	0.1–17	0.2–3	Nieves-Remacha et al. <sup>89</sup>
impinging jet absorber				
conventional	fully mixed	N/A	0.025–1.22	Tamir et al. <sup>93</sup>
high intensity	fully mixed	5–7000	1–14.2	Botes et al.; <sup>94</sup> Siddiqui et al. <sup>56</sup>
monolith loop reactors	co-current	0.5–30	0.05–0.5	Heiszwolf et al.; <sup>95</sup> Vandu et al. <sup>79</sup>
MAT	fully mixed	0.2–20	0.003–0.5	Schlüter and Deckwer; <sup>96</sup> Middleton and Smith <sup>1</sup>
static mixers				
lightening, grid, screen	co-current	0.2–95	0.1–2.3	Roes et al.; <sup>41</sup> Heyouni et al.; <sup>44</sup> Al Taweel et al.; <sup>16</sup> Munter <sup>46</sup>
present investigation	co-current	30–270	0.27–4.08	–

<sup>a</sup>N/A: not available.

equipped with a series of heart-shaped confined sections with obstacles to enhance the continuous breakup and coalescence of bubbles. Higher  $k_L a$  values could thus be achieved at lower local energy dissipation rates and much larger gas and liquid flow rates could be processed in a single unit (up to about 5 L of liquid per hour and gas holdups up to 0.68). Multiple advanced flow reactor (AFR) units operated in parallel can be used to handle larger flow capacities, but the capital costs associated with such an arrangement may be prohibitive.

An example of a system design that relies on passing the two-phase stream through a field of high turbulent intensity is the impinging jet reactor. They depict high throughput capacity (up to 30 L/h), very high  $k_L a$  values, and excellent mixing and have the added advantage that all of the incoming fluid must pass through the maximum energy dissipation zone where  $\epsilon$  values as high as 7000 W/kg can be achieved. The residence times in IJR were found to vary between 40 and 230 ms,<sup>56</sup> depending on the liquid flow which, as shown in section 3.1, suggests that the specific energy consumption per unit mass processed,  $E_{\text{SPM}}$  in such units is expected to be rather low. There is however no indication in the public literature of its use for large-capacity gas–liquid contacting purposes, but multiple units operated in parallel can be used to deal with intermediate flow rates.

Even larger throughputs can be achieved using monolith loop reactors (MLRs) in which the mass transfer in the liquid phase is promoted by surface renewal of the liquid film between a relatively large bubble and the surface of the monolith channel surrounding it. Depending on the size of the monolith channel used, the energy dissipation rate can be quite significant, particularly at large liquid superficial velocities, but the resulting  $k_L a$  values are somewhat limited in comparison to other more effective contactors.

Mechanically agitated tanks are one of the most commonly used gas–liquid contactors with relatively low average energy dissipation rates combined with very high local  $\epsilon$  values at the impeller tips where a significant part of the bubble dispersion takes place. However, their performance suffers from the nonuniform distribution of gas holdup throughout the reactor volume (particularly at low rotational speeds) and complex internal circulation patterns that do not guarantee that all of the incoming fluids must pass through the maximum energy dissipation zone. Proper design and scaleup of such units is therefore rather complex and usually requires the use of advanced computational fluid dynamics and PBE simulations to achieve close correspondence with experimental results.<sup>97,98</sup> Their biggest mass-transfer disadvantage stems from the

extensive internal circulation taking place within such units, which in turn, results in reducing the mass-transfer driving force, particularly when equilibrium conditions are to be approached. All these factors result in large residence times being needed for such units, which consequently increases the capital and operating costs ( $E_t$ ) requirement and the need to recycle the gas if high conversion efficiency of the constituents present in that phase is needed.<sup>81</sup>

On the other hand, static mixers are high-throughput devices that can be applied to a wide range of process operations and offer many key benefits for contacting liquids, gases, and powders. To meet the specific needs of each application, various static mixing element designs (over 50 different designs) have evolved, but the number that have been tested for gas–liquid contacting is rather limited although the mass-transfer coefficients achieved in static mixers can be 2 orders of magnitude higher than that in conventional stirred tanks and bubble columns. The use of static mixers allows for a high degree of flexibility because they can be made from a wide range of materials, they are very compact and can be used in both vertical and horizontal orientation, and their operational characteristics can be easily varied without interruption by changing the gas-to-liquid flow ratios. Although they normally have a limited turndown ratio (because the mixing energy is drawn from the kinetic energy of the pipe flow), this problem can be overcome by using several static mixing lines in parallel.<sup>8</sup>

As shown in Table 2, the gas–liquid mass-transfer performance of screen/grid static mixers surpassed that of most conventional reactor/contactors with more than an order of magnitude difference in the reported  $k_L a$  values. This, in combination with the essentially plug flow characteristics encountered in this contactor, resulted in the ability to reach 98% equilibrium within residence times of less than 800 ms (Figure 15). Shorter times can be reached without significantly increasing the power consumption rates ( $E_t$ ) by using an interscreen spacing smaller than that used in the present investigation (e.g., 20 mm). This is several orders of magnitude smaller than the residence times needed for mechanically agitated tanks and bubble columns and is an order of magnitude shorter than that achieved in the tube-in-tube gas–liquid reactor.<sup>99</sup> Consequently, the amount of oxygen transported per unit energy consumed,  $E_t$ , varied between 0.09 and 0.63 kg O<sub>2</sub>/kWh, depending on the operating conditions and interfacial characteristics of the system. This compares well with submerged diffusers and surface aerators (particularly in the presence of contaminants), and is about 2 orders of

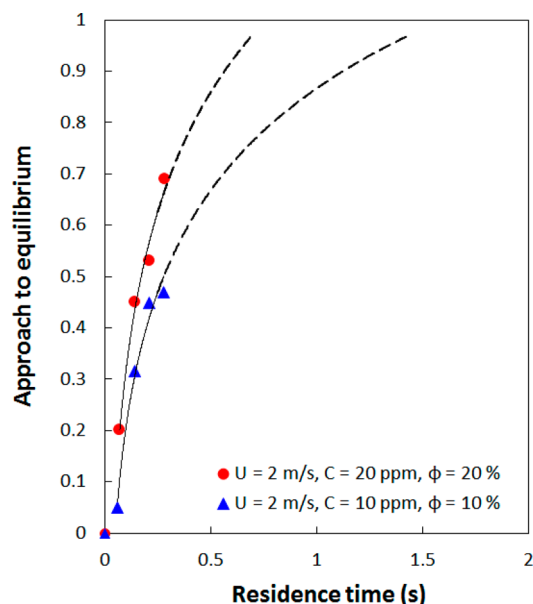


Figure 15. Effect of residence time on the approach to equilibrium.

magnitude higher than that achieved using AFR under the conditions which yield comparably high  $k_L a$  values.<sup>81</sup>

The high energy utilization efficiencies achieved in the screen/grid static mixers can be mainly attributed to the plug flow conditions, very short residence times encountered in this design, the virtual absence of deadzones, and the ability to focus energy dissipation within a small volume in order to generate large interfacial area of contact that slowly diminishes downstream. This is very much along the lines proposed by Kastánek et al.<sup>23</sup> for slowly coalescent systems; however, this approach can be disadvantageous in the case of shear-sensitive systems such as those containing live cells which can be easily damaged and experience high mortality rates. On the other hand, it can be very effective tool for cell lysis.

#### 4. CONCLUSIONS

The volumetric mass-transfer coefficient achieved using a screen/grid-type static mixing element was investigated over a wide range of superficial gas and liquid velocities using gas–liquid systems with three levels of bubble coalescence rates. A modified measurement and interpretation technique was used to enhance the reproducibility of the results and to account for the depletion effect which becomes critical at high mass-transfer rates. The volumetric mass-transfer coefficient,  $k_L a$ , was found to increase with increasing liquid superficial velocity and gas volume fraction and reached values as high as  $4.08 \text{ s}^{-1}$  at low specific energy consumption rates particularly for slowly coalescent systems, a situation that is similar to that encountered in most industrially relevant systems. This high mass-transfer coefficient is expected to improve the selectivity and yield of high-rate multiphase reactions.

This excellent performance can be attributed to the two-phase stream being forced to flow through a succession of very thin high energy dissipation zones where  $\epsilon$  values as high as  $39\,775 \text{ W/kg}$  can be achieved. However, the extremely short residence times in these zones ( $145\text{--}290 \mu\text{s}$ ) results in the energy dissipation rates per unit mass of the streams processed being small ( $0.004\text{--}0.022 \text{ kWh/tonne}$ ) while maintaining high energy utilization efficiency (up to  $0.63 \text{ kg O}_2/\text{kWh}$ ). The high mass-transfer rates achieved in this contactor were further

enhanced by the plug flow conditions prevalent in both phases (which yields a high average mass-transfer driving force).

By repetitively exposing the flowing gas–liquid dispersion to zones of high and low energy dissipation rates, this reactor/contactor was able to take advantage of the coalescence retardation characteristics of most industrially relevant streams and achieve  $k_L a$  values that surpassed those of most conventional reactors/contactors by an order of magnitude. The ability to reach 98% equilibrium within residence times of less than 800 ms also allows for the use of static mixing units that are several orders of magnitude smaller than conventional units such as mechanically agitated tanks and bubble columns.

#### ■ ASSOCIATED CONTENT

##### Supporting Information

The Supporting Information is available free of charge on the ACS Publications website at DOI: 10.1021/acs.iecr.5b01078.

Tables providing the characteristics of the stainless steel plain-weave wire cloth used, physical properties of systems investigated, and range of experimental conditions investigated (PDF)

#### ■ AUTHOR INFORMATION

##### Corresponding Author

\*E-mail: al.taweel@dal.ca.

##### Notes

The authors declare no competing financial interest.

#### ■ ACKNOWLEDGMENTS

The financial support of the Natural Sciences and Engineering Research Council of Canada (NSERC), Dalhousie University, and the American University of Beirut, through its University Research Board (URB), is gratefully acknowledged.

#### ■ NOMENCLATURE

- $a$  = Interfacial area of contact [ $\text{m}^2/\text{m}^3$ ]
- $b$  = Screen wire diameter [m]
- $C$  = Bulk surfactant concentration [ppm]
- $C_{\text{O}_2}^*$  = Oxygen concentration in liquid phase at equilibrium [ppm]
- $C_{\text{O}_2}$  = Oxygen concentration in liquid phase [ppm]
- $D$  = Diffusivity [ $\text{m}^2/\text{s}$ ]
- $D$  = Pipe diameter or tank diameter [m]
- $E$  = Energy dissipation rate [kW]
- $E_m$  = Energy dissipation per unit mass of the liquid [ $\text{W/kg}$ ]
- $E_v$  = Energy dissipation per unit of the reactor volume [ $\text{kW}/\text{m}^3$ ]
- $E_{\text{spm}}$  = Specific energy consumption rate per unit mass of liquid processed [ $\text{kW/kg}$ ]
- $E_t$  = The amount of oxygen transported to or from liquid phase per unit of energy dissipated [ $\text{kg O}_2/\text{kWh}$ ]
- $k_L$  = Mass-transfer coefficient [ $\text{m s}^{-1}$ ]
- $k_L a$  = Volumetric mass-transfer coefficient [ $\text{s}^{-1}$ ]
- $L$  = Pipe length [m]
- $L_M$  = Length of the mixing section [m]
- $L_{\text{screen}}$  = Interscreen spacing in the mixing section [m]
- $M$  = Wire mesh size [m]
- $M_{\text{O}_2}$  = The amount of oxygen exchanged between the gas and liquid phases [ $\text{kg/h}$ ]
- $n_{\text{O}_2}$  = Number of moles of Oxygen [g mol]
- $n_{\text{N}_2}$  = Number of moles of Nitrogen [g mol]
- $Q$  = Volumetric flow rate [ $\text{m}^3/\text{s}$ ]

Re = Pipe Reynolds number [–]  
 Re<sub>w</sub> = Wire Reynolds number [–]  
 t = Residence time [s]  
 U = Superficial velocity [m/s]  
 V = Volume [m<sup>3</sup>]

### Greek Symbols

$\alpha$  = Porosity or percentage open area of screen  
 $\Delta P$  = Pressure drop in the pipe [Pa]  
 $\varepsilon$  = Turbulent kinetic energy dissipation rate [W/kg]  
 $\rho$  = Density [kg/m<sup>3</sup>]  
 $\sigma$  = Static (equilibrium) surface tension [mN/m]  
 $\mu$  = Viscosity [cP]  
 $\phi$  = Volumetric fraction of dispersed phase [–]  
 $\Pi$  = Surface pressure [mN/m]

### Subscripts

c = Continuous phase  
 G = Gas  
 L = Liquid  
 avg. = Average  
 max = Maximum  
 min = Minimum  
 mix = Mixture properties  
 rem = Moles remaining  
 trans = Moles transferred

## REFERENCES

- Middleton, J. C.; Smith, J. M. Gas–liquid Mixing in Turbulent Systems. *Handbook of Industrial Mixing: Science and Practice* **2003**, 585.
- Laakkonen, M.; Alopaeus, V.; Aittamaa, J. Validation of Bubble Breakage, Coalescence and Mass Transfer Models for Gas–liquid Dispersion in Agitated Vessel. *Chem. Eng. Sci.* **2006**, *61*, 218.
- Zhang, J.; Xu, S.; Li, W. High Shear Mixers: A Review of Typical Applications and Studies on Power Draw, Flow Pattern, Energy Dissipation and Transfer Properties. *Chem. Eng. Process.* **2012**, *57*, 25.
- Boodhoo, K.; Harvey, A. Process Intensification: An Overview of Principles and Practice. In *Process Intensification for Green Chemistry: Engineering Solutions for Sustainable Chemical Processing*; Boodhoo, K., Harvey, A., Eds.; John Wiley & Sons, Ltd.: Chichester, 2013; pp 1–31.
- Andersson, R.; Andersson, B.; Chopard, F.; Norén, T. Development of a Multi-Scale Simulation Method for Design of Novel Multiphase Reactors. *Chem. Eng. Sci.* **2004**, *59*, 4911.
- Thakur, R. K.; Vial, C.; Nigam, K. D. P.; Nauman, E. B.; Djelveh, G. Static Mixers in the Process Industries - a Review. *Chem. Eng. Res. Des.* **2003**, *81*, 787.
- Peschel, A.; Hentschel, B.; Freund, H.; Sundmacher, K. Design of Optimal Multiphase Reactors Exemplified on the Hydroformylation of Long Chain Alkenes. *Chem. Eng. J.* **2012**, *188*, 126.
- Al Taweel, A. M.; Azizi, F.; Sirijeerachai, G. Static Mixers: Effective Means for Intensifying Mass Transfer Limited Reactions. *Chem. Eng. Process.* **2013**, *72*, 51.
- Ghanem, A.; Lemenand, T.; Della Valle, D.; Peerhossaini, H. Static Mixers: Mechanisms, Applications, and Characterization methods—A Review. *Chem. Eng. Res. Des.* **2014**, *92*, 205.
- Chen, C. *Dispersion and Coalescence in Static Mixers*. Ph.D. Thesis, Technical University of Nova Scotia, 1996.
- Al Taweel, A. M.; Chen, C. Novel Static Mixer for the Effective Dispersion of Immiscible Liquids. *Chem. Eng. Res. Des.* **1996**, *74*, 445.
- Bourne, J. R. R.; Lips, M. Micromixing in Grid-Generated Turbulence. Theoretical Analysis and Experimental Study. *Chem. Eng. J. Biochem. Eng. J.* **1991**, *47*, 155.
- Azizi, F.; Al Taweel, A. M. Inter-Phase Mass Transfer in Turbulent Liquid-Liquid Dispersions: A Comparative Analysis of Models. *Chem. Eng. J.* **2012**, *179*, 231.
- Al Taweel, A. M.; Li, C.; Gomaa, H. G.; Yuet, P. Intensifying Mass Transfer between Immiscible Liquids: Using Screen-Type Static Mixers. *Chem. Eng. Res. Des.* **2007**, *85*, 760.
- Hweij, K. A.; Azizi, F. Hydrodynamics and Residence Time Distribution of Liquid Flow in Tubular Reactors Equipped with Screen-Type Static Mixers. *Chem. Eng. J.* **2015**, *279*, 948.
- Al Taweel, A. M.; Yan, J.; Azizi, F.; Odedra, D.; Gomaa, H. G. Using in-Line Static Mixers to Intensify Gas–liquid Mass Transfer Processes. *Chem. Eng. Sci.* **2005**, *60*, 6378.
- Davies, J. T. *Turbulence Phenomena*; Academic Press: New York, 1972.
- Walter, J. F.; Blanch, H. W. Bubble Break-up in Gas-Liquid Bioreactors: Break-up in Turbulent Flows. *Chem. Eng. J. Biochem. Eng. J.* **1986**, *32*, B7.
- Hinze, J. O. Fundamentals of the Hydrodynamic Mechanism of Splitting in Dispersion Processes. *AIChE J.* **1955**, *1*, 289.
- Grau, R. A.; Laskowski, J. S. Role of Frothers in Bubble Generation and Coalescence in a Mechanical Flotation Cell. *Can. J. Chem. Eng.* **2006**, *84*, 170.
- Azizi, F.; Al Taweel, A. M. Population Balance Simulation of Gas-Liquid Contacting. *Chem. Eng. Sci.* **2007**, *62* (24), 7436.
- Camarasa, E.; Vial, C.; Poncin, S.; Wild, G.; Midoux, N.; Bouillard, J. Influence of Coalescence Behaviour of the Liquid and of Gas Sparging on Hydrodynamics and Bubble Characteristics in a Bubble Column. *Chem. Eng. Process.* **1999**, *38*, 329.
- Kastánek, F.; Zahradník, J.; Kratochvíl, J.; Cermák, J. *Chemical Reactors for Gas-Liquid Systems*; Ellis Horwood: New York, 1993; ISBN-13: 978-0131273900.
- Vakarelski, I. U.; Manica, R.; Tang, X.; O'Shea, S. J.; Stevens, G. W.; Grieser, F.; Dagastine, R. R.; Chan, D. Y. Dynamic Interactions between Microbubbles in Water. *Proc. Natl. Acad. Sci. U. S. A.* **2010**, *107*, 11177.
- Vazquez, G.; Antorrena, G.; Navaza, J. M. Influence of Surfactant Concentration and Chain Length on the Absorption of CO<sub>2</sub> by Aqueous Surfactant Solutions in the Presence and Absence of Induced Marangoni Effect. *Ind. Eng. Chem. Res.* **2000**, *39*, 1088.
- Vasconcelos, J. M. T.; Orvalho, S. P.; Alves, S. S. S. Gas-Liquid Mass Transfer to Single Bubbles: Effect of Surface Contamination. *AIChE J.* **2002**, *48*, 1145.
- Alves, S. S. S.; Maia, C. I. I.; Vasconcelos, J. M. T. M. T. Gas-Liquid Mass Transfer Coefficient in Stirred Tanks Interpreted through Bubble Contamination Kinetics. *Chem. Eng. Process.* **2004**, *43*, 823.
- Rosso, D.; Huo, D. L.; Stenstrom, M. K. Effects of Interfacial Surfactant Contamination on Bubble Gas Transfer. *Chem. Eng. Sci.* **2006**, *61*, 5500.
- Hebrard, G.; Zeng, J.; Loubiere, K. Effect of Surfactants on Liquid Side Mass Transfer Coefficients: A New Insight. *Chem. Eng. J.* **2009**, *148*, 132.
- McKenna, S. P.; McGillis, W. R. The Role of Free-Surface Turbulence and Surfactants in Air–water Gas Transfer. *Int. J. Heat Mass Transfer* **2004**, *47*, 539.
- Painmanakul, P.; Loubière, K.; Hébrard, G.; Mietton-Peuchot, M.; Roustan, M. Effect of Surfactants on Liquid-Side Mass Transfer Coefficients. *Chem. Eng. Sci.* **2005**, *60*, 6480.
- Al-Masry, W. A. Effects of Antifoam and Scale-up on Operation of Bioreactors. *Chem. Eng. Process.* **1999**, *38*, 197.
- Linek, V.; Kordač, M.; Moucha, T. Mechanism of Mass Transfer from Bubbles in Dispersions Part II: Mass Transfer Coefficients in Stirred Gas-Liquid Reactor and Bubble Column. *Chem. Eng. Process.* **2005**, *44*, 121.
- Zlokarnik, M. Tower-Shaped Reactors for Aerobic Biological Waste Water Treatment. *Biotechnology* **1985**, *2*, 537.
- Merchuk, J. C.; Contreras, A.; Garcia, F.; Molina, E. Studies of Mixing in a Concentric Tube Airlift Bioreactor with Different Spargers. *Chem. Eng. Sci.* **1998**, *53*, 709.
- Al Taweel, A. M.; Cheng, Y. H. Effect of Surface Tension on Gas/liquid Contacting in a Mechanically-Agitated Tank with Stator. *Chem. Eng. Res. Des.* **1995**, *73*, 654.
- Kluytmans, J. H. J.; van Wachem, B. G. M.; Kuster, B. F. M.; Schouten, J. C. Gas Holdup in a Slurry Bubble Column: Influence of Electrolyte and Carbon Particles. *Ind. Eng. Chem. Res.* **2001**, *40*, 5326.

- (38) Garcia-Ochoa, F.; Gomez, E. Bioreactor Scale-up and Oxygen Transfer Rate in Microbial Processes: An Overview. *Biotechnol. Adv.* **2009**, *27*, 153.
- (39) Šijački, I. M.; Tokić, M. S.; Kojić, P. S.; Petrović, D. L.; Tekić, M. N.; Djurić, M. S.; Milovančević, S. S. Sparger Type Influence on the Hydrodynamics of the Draft Tube Airlift Reactor with Diluted Alcohol Solutions. *Ind. Eng. Chem. Res.* **2011**, *50*, 3580.
- (40) Gaddis, E. S. Mass Transfer in Gas-liquid Contactors. *Chem. Eng. Process.* **1999**, *38*, 503.
- (41) Jiang, P.; Stenstrom, M. K. Oxygen Transfer Parameter Estimation: Impact of Methodology. *J. Environ. Eng.* **2012**, *138*, 137.
- (42) Roes, A. W. M.; Zeeman, A. J.; Bukkems, F. H. J. High Intensity Gas/Liquid Mass Transfer in the Bubbly Flow Region during Co-Current Upflow through Static Mixers. *ICHEME Symp. Ser.* **1984**, *87*, 231.
- (43) Turunen, I.; Haario, H. Mass Transfer in Tubular Reactors Equipped with Static Mixers. *Chem. Eng. Sci.* **1994**, *49*, 5257.
- (44) Heyouni, A.; Roustan, M.; Do-quang, Z. Hydrodynamics and Mass Transfer in Gas-liquid Flow through Static Mixers. *Chem. Eng. Sci.* **2002**, *57*, 3325.
- (45) Sanchez, C.; Couvert, A.; Laplanche, A.; Renner, C. Hydrodynamic and Mass Transfer in a New Co-Current Two-Phase Flow Gas-liquid Contactor. *Chem. Eng. J.* **2007**, *131*, 49.
- (46) Munter, R. Comparison of Mass Transfer Efficiency and Energy Consumption in Static Mixers. *Ozone: Sci. Eng.* **2010**, *32*, 399.
- (47) Stenstrom, M. K.; Gilbert, R. G. Effects of Alpha, Beta and Theta Factor upon the Design, Specification and Operation of Aeration Systems. *Water Res.* **1981**, *15*, 643.
- (48) Wagner, M.; Pöpel, H. J. Surface Active Agents and Their Influence on Oxygen Transfer. *Water Sci. Technol.* **1996**, *34*, 249.
- (49) Zahradník, J.; Fialova, M.; Linek, V. The Effect of Surface-Active Additives on Bubble Coalescence in Aqueous Media. *Chem. Eng. Sci.* **1999**, *54*, 4757.
- (50) Luo, J. J. Bubble Dispersion and Coalescence in Turbulent Pipe Flow. Ph.D. Thesis, Dalhousie University, 2002.
- (51) Ziolkowski, D.; Morawski, J. The Flow Characteristic of the Liquid Streams inside a Tubular Apparatus Equipped with Static Mixing Elements of a New Type. *Chem. Eng. Process.* **1987**, *21*, 131.
- (52) Staudinger, J.; Roberts, P. V. A Critical Compilation of Henry's Law Constant Temperature Dependence Relations for Organic Compounds in Dilute Aqueous Solutions. *Chemosphere* **2001**, *44*, 561.
- (53) Azizi, F.; Al Taweel, A. M. Hydrodynamics of Liquid Flow Through Screens and Screen-Type Static Mixers. *Chem. Eng. Commun.* **2011**, *198*, 726.
- (54) Azizi, F.; Al Taweel, A. M. Turbulently Flowing Liquid-liquid Dispersions. Part I: Drop Breakage and Coalescence. *Chem. Eng. J.* **2011**, *166*, 715.
- (55) Zhou, G.; Kresta, S. M. Correlation of Mean Drop Size and Minimum Drop Size with the Turbulence Energy Dissipation and the Flow in an Agitated Tank. *Chem. Eng. Sci.* **1998**, *53*, 2063.
- (56) Siddiqui, S. W.; Zhao, Y.; Kukukova, A.; Kresta, S. M. Characteristics of a Confined Impinging Jet Reactor: Energy Dissipation, Homogeneous and Heterogeneous Reaction Products, and Effect of Unequal Flow. *Ind. Eng. Chem. Res.* **2009**, *48*, 7945.
- (57) Micheletti, M.; Baldi, S.; Yeoh, S. L.; Ducci, A.; Papadakis, G.; Lee, K. C.; Yianneskis, M. On Spatial and Temporal Variations and Estimates of Energy Dissipation in Stirred Reactors. *Chem. Eng. Res. Des.* **2004**, *82*, 1188.
- (58) Koglin, B.; Pawlowski, J.; Schnöring, H. Kontinuierliches Emulgieren Mit Rotor/Stator-Maschinen: Einfluß Der Volumenbezogenen Dispergierleistung Und Der Verweilzeit Auf Die Emulsionsfeinheit. *Chem. Ing. Tech.* **1981**, *53*, 641.
- (59) Al Taweel, A. M.; Walker, L. D. Liquid Dispersion in Static in-Line Mixers. *Can. J. Chem. Eng.* **1983**, *61*, 527.
- (60) Schubert, H.; Engel, R. Product and Formulation Engineering of Emulsions. *Chem. Eng. Res. Des.* **2004**, *82*, 1137.
- (61) Kuzmin, A. O.; Pravdina, M. K.; Yavorsky, A. I.; Yavorsky, N. I.; Parmon, V. N. Vortex Centrifugal Bubbling Reactor. *Chem. Eng. J.* **2005**, *107*, 55.
- (62) Cancino, B.; Roth, P.; Reuß, M. Design of High Efficiency Surface Aerators: Part 1. Development of New Rotors for Surface Aerators. *Aquac. Eng.* **2004**, *31*, 83.
- (63) Stenstrom, M. K.; Leu, S. Y.; Jiang, P. Theory to Practice: Oxygen Transfer and the New ASCE Standard. *Proc. Water Environ. Fed.* **2006**, *2006*, 4838.
- (64) Li, H. Z.; Fasol, C.; Choplin, L. Pressure Drop of Newtonian and Non-Newtonian Fluids across a Sulzer SMX Static Mixer. *Chem. Eng. Res. Des.* **1997**, *75*, 792.
- (65) Kumar, V.; Shirke, V.; Nigam, K. D. P. Performance of Kenics Static Mixer over a Wide Range of Reynolds Number. *Chem. Eng. J.* **2008**, *139*, 284.
- (66) Zirrahi, M.; Hassanzadeh, H.; Abedi, J. The Laboratory Testing and Scale-up of a Downhole Device for CO<sub>2</sub> Dissolution Acceleration. *Int. J. Greenhouse Gas Control* **2013**, *16*, 41.
- (67) Parmar, R.; Majumder, S. K. Hydrodynamics of Microbubble Suspension Flow in Pipes. *Ind. Eng. Chem. Res.* **2014**, *53*, 3689.
- (68) Zhen, L.; Hassan, Y. A. Wavelet Autocorrelation Identification of the Turbulent Flow Multi-Scales for Drag Reduction Process in Microbubbly Flows. *Chem. Eng. Sci.* **2006**, *61*, 7107.
- (69) Pang, M.; Wei, J. Experimental Investigation on the Turbulence Channel Flow Laden with Small Bubbles by PIV. *Chem. Eng. Sci.* **2013**, *94*, 302.
- (70) Ceccio, S. L. Friction Drag Reduction of External Flows with Bubble and Gas Injection. *Annu. Rev. Fluid Mech.* **2010**, *42*, 183.
- (71) Nouri, N. M.; Motlagh, S. Y.; Navidbakhsh, M.; Dalilhaghi, M.; Moltani, A. A. Bubble Effect on Pressure Drop Reduction in Upward Pipe Flow. *Exp. Therm. Fluid Sci.* **2013**, *44*, 592.
- (72) Ehrhardt, G. Flow Measurements for Wire Gauzes. *Int. Chem. Eng.* **1983**, *23*, 455.
- (73) Martín, M.; Montes, F. J.; Galán, M. A. Physical Explanation of the Empirical Coefficients of Gas-liquid Mass Transfer Equations. *Chem. Eng. Sci.* **2009**, *64*, 410.
- (74) Moucha, T.; Rejl, F. J.; Kordač, M.; Labík, L. Mass Transfer Characteristics of Multiple-Impeller Fermenters for Their Design and Scale-Up. *Biochem. Eng. J.* **2012**, *69*, 17.
- (75) Lezhnin, S.; Eskin, D.; Leonenko, Y.; Vinogradov, O. Dissolution of Air Bubbles in a Turbulent Water Pipeline Flow. *Heat Mass Transfer* **2003**, *39*, 483.
- (76) Linek, V.; Kordač, M.; Fújasová, M.; Moucha, T. Gas-liquid Mass Transfer Coefficient in Stirred Tanks Interpreted through Models of Idealized Eddy Structure of Turbulence in the Bubble Vicinity. *Chem. Eng. Process.* **2004**, *43*, 1511.
- (77) Letzel, H. M.; Schouten, J. C.; Krishna, R.; van den Bleek, C. M. Characterization of Regimes and Regime Transitions in Bubble Columns by Chaos Analysis of Pressure Signals. *Chem. Eng. Sci.* **1997**, *52*, 4447.
- (78) Vandu, C. O.; Krishna, R. Volumetric Mass Transfer Coefficients in Slurry Bubble Columns Operating in the Churn-Turbulent Flow Regime. *Chem. Eng. Process.* **2004**, *43*, 987.
- (79) Vandu, C. O.; Ellenberger, J.; Krishna, R. Hydrodynamics and Mass Transfer in an Upflow Monolith Loop Reactor. *Chem. Eng. Process.* **2005**, *44*, 363.
- (80) van der Schaaf, J.; Chilekar, V. P.; van Ommen, J. R.; Kuster, B. F. M.; Tinge, J. T.; Schouten, J. C. Effect of Particle Lyophobicity in Slurry Bubble Columns at Elevated Pressures. *Chem. Eng. Sci.* **2007**, *62*, 5533.
- (81) Al Taweel, A. M.; Azizi, F.; Yang, J. Energy Utilization Efficiency in Gas-Liquid Contacting. In Book of Full-length Manuscripts, 2nd International Symposium on Multiscale Multiphase Process Engineering MMPE, Hamburg, Sept. 24-27, 2014; DECHEMA e.V.: Frankfurt, 2014; p 154.
- (82) Majirova, H.; Pinelli, D.; Machon, V.; Magelli, F. Gas Flow Behavior in a Two-Phase Reactor Stirred with Triple Turbines. *Chem. Eng. Technol.* **2004**, *27*, 304.
- (83) Jackson, M. L. Aeration in Bernoulli Types of Devices. *AIChE J.* **1964**, *10*, 836.

(84) Koide, K.; Yamazoe, S.; Harada, S. Effects of Surface-Active Substance on Gas Holdup and Gas-Liquid Mass Transfer in Bubble Column. *J. Chem. Eng. Jpn.* **1985**, *18*, 287.

(85) Vasconcelos, J. M. T.; Rodrigues, J. M. L.; Orvalho, S. C. P.; Alves, S. S.; Mendes, R. L.; Reis, A. Effect of Contaminants on Mass Transfer Coefficients in Bubble Column and Airlift Contactors. *Chem. Eng. Sci.* **2003**, *58*, 1431.

(86) Sardeing, R.; Painmanakul, P.; Hébrard, G. Effect of Surfactants on Liquid-Side Mass Transfer Coefficients in Gas-liquid Systems: A First Step to Modeling. *Chem. Eng. Sci.* **2006**, *61*, 6249.

(87) Middleton, J. C. Motionless Mixers as Gas Liquid Contacting Devices. Presented at the AIChE 71st Annual Meeting, Miami Beach, FL, November 1978; Paper 74e.

(88) Linek, V.; Moucha, T.; Rejl, F. J.; Kordač, M.; Hovorka, F.; Opletal, M.; Haidl, J. Power and Mass Transfer Correlations for the Design of Multi-Impeller Gas-liquid Contactors for Non-Coalescent Electrolyte Solutions. *Chem. Eng. J.* **2012**, *209*, 263.

(89) Nieves-Remacha, M. J.; Kulkarni, A. A.; Jensen, K. F. Gas-Liquid Flow and Mass Transfer in an Advanced-Flow Reactor. *Ind. Eng. Chem. Res.* **2013**, *52*, 8996.

(90) Martin, N.; Benezet-Toulze, M.; Laplace, C.; Faivre, M.; Langlais, B. Design And Efficiency Of Ozone Contactors For Disinfection. *Ozone: Sci. Eng.* **1992**, *14*, 391.

(91) Yue, J.; Chen, G.; Yuan, Q.; Luo, L.; Gonthier, Y. Hydrodynamics and Mass Transfer Characteristics in Gas-liquid Flow through a Rectangular Microchannel. *Chem. Eng. Sci.* **2007**, *62*, 2096.

(92) Meeuwse, M.; van der Schaaf, J.; Kuster, B. F. M.; Schouten, J. C. Gas-liquid Mass Transfer in a Rotor-stator Spinning Disc Reactor. *Chem. Eng. Sci.* **2010**, *65*, 466.

(93) Tamir, A.; Herskowitz, D.; Herskowitz, V. Impinging Jet Absorbers. *Chem. Eng. Process.* **1990**, *28*, 165.

(94) Botes, F. G.; Lorenzen, L.; van Deventer, J. S. J. The Development of High Intensity Gas-Liquid Jet Reactors. *Chem. Eng. Commun.* **1998**, *170*, 217.

(95) Heiszwolf, J. J.; Engeltaart, L. B.; van den Eijnden, M.; Kreutzer, M. T.; Kapteijn, F.; Moulijn, J. A. Hydrodynamic Aspects of the Monolith Loop Reactor. *Chem. Eng. Sci.* **2001**, *56*, 805.

(96) Schlüter, V.; Deckwer, W.-D. Gas/liquid Mass Transfer in Stirred Vessels. *Chem. Eng. Sci.* **1992**, *47*, 2357.

(97) Alopaeus, V.; Laakkonen, M.; Aittamaa, J. Solution of Population Balances with Growth and Nucleation by High Order Moment-Conserving Method of Classes. *Chem. Eng. Sci.* **2007**, *62*, 2277.

(98) Petitti, M.; Vanni, M.; Marchisio, D. L.; Buffo, A.; Podenzani, F. Simulation of Coalescence, Break-up and Mass Transfer in a Gas-liquid Stirred Tank with CQMOM. *Chem. Eng. J.* **2013**, *228*, 1182.

(99) Yang, L.; Jensen, K. F. Mass Transport and Reactions in the Tube-in-Tube Reactor. *Org. Process Res. Dev.* **2013**, *17*, 927.